

SHED: A Newton-type algorithm for federated learning based on incremental Hessian eigenvector sharing

Nicolò Dal Fabbro

*Department of Information Engineering
University of Padova
Padova, PD 35122, Italy*

NICOLO.DALFABBRO@STUDENTI.UNIPD.IT

Subhrakanti Dey

*Department of Electrical Engineering
Uppsala University
Uppsala, 751 03, Sweden*

SUBHRAKANTI.DEY@ANGSTROM.UU.SE

Michele Rossi

*Department of Information Engineering
University of Padova
Padova, PD 35122, Italy*

MICHELE.ROSSI@UNIPD.IT

Luca Schenato

*Department of Information Engineering
University of Padova
Padova, PD 35122, Italy*

SCHENATO@DEI.UNIPD.IT

Abstract

There is a growing interest in the distributed optimization framework that goes under the name of Federated Learning (FL). In particular, much attention is being turned to FL scenarios where the network is strongly heterogeneous in terms of communication resources (e.g., bandwidth) and data distribution. In these cases, communication between local machines (*agents*) and the central server (*Master*) is a main consideration. In this work, we present SHED¹, an original communication-constrained Newton-type (NT) algorithm designed to accelerate FL in such heterogeneous scenarios. SHED is by design robust to non i.i.d. data distributions, handles heterogeneity of agents' communication resources (CRs), only requires sporadic Hessian computations, and achieves super-linear convergence. This is possible thanks to an *incremental* strategy, based on eigendecomposition of the local Hessian matrices, which exploits (possibly) *outdated* second-order information. The proposed solution is thoroughly validated on real datasets by assessing (i) the number of communication rounds required for convergence, (ii) the overall amount of data transmitted and (iii) the number of local Hessian computations. For all these metrics, the proposed approach shows superior performance against state-of-the-art techniques like GIANT and FedNL.

Keywords: Federated learning, Newton method, distributed optimization, heterogeneous networks, edge learning, non i.i.d. data.

1. In a previous preprint version of this paper, the algorithm was referred to as IOS

1. Introduction

With the growing computational power of edge devices and the booming increase of data produced and collected by users worldwide, solving machine learning problems without having to collect data at a central server is becoming very appealing (Shi et al., 2020). One of the main reasons for not transferring users’ data to cloud central servers is due to privacy concerns. Indeed, users, such as individuals or companies, may not want to share their private data with other network entities, while training their machine learning algorithms. In addition to privacy, distributed processes are by nature more resilient to node/link failures and can be directly implemented on the servers at network edge, i.e., within multi-access edge computing (MEC) scenarios (Pham et al., 2020).

This distributed learning framework goes under the name of federated learning (FL) (McMahan et al., 2017; Li et al., 2020a), and it has attracted much research interest in recent years. Direct applications of FL can be found, for example, in the field of healthcare systems (Rieke et al., 2020; Huang et al., 2020) or of smartphone utilities (Hard et al., 2018).

One of the most popular FL algorithms is federated averaging (FedAvg) (McMahan et al., 2017), which achieves good results, but which comes with weak convergence guarantees and has been shown to diverge under heterogeneous data distributions (Li et al., 2020b).

Indeed, among the open challenges of FL, a key research question is how to provide efficient distributed optimization algorithms in scenarios with heterogeneous communication links (different bandwidth) and non i.i.d. data distributions (Kairouz et al., 2021; Zhu et al., 2021; Smith et al., 2017; Zhao et al., 2018). These aspects are found in a variety of applications, such as the so-called *federated edge learning* framework, where learning is moved to the network edge, and which often involves unstable and heterogeneous wireless connections (Shi et al., 2020; T. Dinh et al., 2022; Nguyen et al., 2021; Chen et al., 2020). In addition, the MEC and FL paradigms are of high interest to IoT scenarios such as data retrieval and processing within smart cities, which naturally entail non i.i.d. data distributions due to inherent statistical differences in the underlying spatial processes (e.g., vehicular mobility, user density, etc.) (Liu et al., 2020).

The bottleneck represented by communication overhead is one of the most critical aspects of FL. In fact, in scenarios with massive number of devices involved, inter-agent communication can be much slower than the local computations performed by the FL agents themselves (e.g., the edge devices), by many orders of magnitude (Li et al., 2020a). The problem of reducing the communication overhead of FL becomes even more critical when the system is characterized by non i.i.d. data distributions and heterogeneous communication resources (CRs) (Li et al., 2020b). In this setting, where the most critical aspect is inter-node communications, FL agents are usually assumed to have good computing capabilities, and wisely increasing the computation effort at the agents is a good strategy to obtain a faster convergence. For this reason, Newton-type approaches, characterized by strong robustness and fast convergence rates, even if computationally demanding, have been recently advocated (Gupta et al., 2021; Safaryan et al., 2021).

In the present work, we present SHED (Sharing Hessian Eigenvectors for distributed learning), a Newton-type FL framework that is naturally robust to non i.i.d. data distri-

butions and that intelligently allocates the (per-iteration) communication resources of the involved FL agents, allowing those with more CRs to contribute more towards improving the convergence rate. Differently from prior art, SHED requires FL agents to locally compute the Hessian matrix sporadically. Its super-linear convergence is here proven by studying the CRs-dependent convergence rate of the algorithm by analyzing the dominant Lyapunov exponent of the estimation error. With respect to other Newton-type methods for distributed learning, our empirical results demonstrate that the proposed framework is (i) competitive with state-of-the-art approaches in i.i.d. scenarios and (ii) robust to non i.i.d. data distributions, for which it outperforms competing solutions.

1.1 Related work

Next, to put our contribution into context, we review previous related works on first and second order methods for distributed learning.

First-order methods. Some methods have been recently proposed to tackle non i.i.d. data and heterogeneous networks. SCAFFOLD (Karimireddy et al., 2020), FedProx (Li et al., 2020b) and the work in Yu et al. (2019) propose modifications to the FedAvg algorithm to face system’s heterogeneity. To deal with non i.i.d. datasets, strategies like those in Zhao et al. (2018) and Jeong et al. (2018) have been put forward, although these approaches require that some data is shared with the central server, which does not fit the privacy requirements of FL. To reduce the FL communication overhead, the work in Chen et al. (2018) leverages the use of outdated first-order information by designing simple rules to detect slowly varying local gradients. With respect to heterogeneous time-varying CRs problem, Amiri and Gündüz (2020) presented techniques based on gradient quantization and on analog communication strategies exploiting the additive nature of the wireless channel, while Chen et al. (2020) studied a framework to jointly optimize learning and communication for FL in wireless networks.

Second-order methods. Newton-type (NT) methods exploit second-order information of the cost function to provide accelerated optimization, and are therefore appealing candidates to speed up FL. NT methods have been widely investigated for distributed learning purposes: GIANT (Wang et al., 2018) is an NT approach exploiting the harmonic mean of local Hessian matrices in distributed settings. Other related techniques are LocalNewton (Gupta et al., 2021), DANE (Shamir et al., 2014), AIDE (Reddi et al., 2016), DiSCO (Zhang and Lin, 2015), DINGO (Crane and Roosta, 2019) and DANLA (Zhang et al., 2022). DONE (T. Dinh et al., 2022) is another technique inspired by GIANT and specifically designed to tackle federated edge learning scenarios. Communication efficient NT methods like GIANT and DONE exploit an extra communication round to obtain estimates of the global Hessian from the harmonic mean of local Hessian matrices. These algorithms, however, were all designed assuming that data is i.i.d. distributed across agents and, as we empirically show in this paper, under-perform if such assumption does not hold. A recent study, FedNL (Safaryan et al., 2021), proposed algorithms based on matrix compression which use theory developed in Islamov et al. (2021) to perform distributed training, by iteratively learning the Hessian matrix at the optimum. A similar approach based on matrix compression techniques has been considered in Basis Learn (Qian et al., 2021), proposing variants of FedNL that exploit change of basis in the space of matrices to improve the quality of the compressed

Hessian. However, these solutions do not consider heterogeneity in the CRs, and require the computation of the local Hessian at each iteration. Another NT technique has been recently proposed in Liu et al. (2021), based on the popular L-BFGS (Liu and Nocedal, 1989) quasi-Newton method. Other recent related NT approaches have been proposed in FLECS (Agafonov et al., 2022), FedNew (Elgabli et al., 2022) and Quantized Newton (Almisis et al., 2021). Although some preliminary NT approaches have been proposed for the FL framework, there is still large space for improvements especially in ill-conditioned setups with heterogeneous CRs and non i.i.d. data distributions.

1.2 Contribution

In this work, we design SHED (Sharing Hessian Eigenvectors for Distributed learning), a communication-constrained NT optimization algorithm for FL that is suitable for networks with heterogeneous CRs and non i.i.d. data. SHED requires only sporadic Hessian computation and it is shown to accelerate convergence of convex federated learning problems, reducing communication rounds and communication load in networks with heterogeneous CRs and non i.i.d. data distributions.

In SHED, local machines, the *agents*, compute the local Hessian and its eigendecomposition. Then, according to their available communication resources (CRs), agents share some of the most *relevant* Hessian eigenvector-eigenvalue pairs (EEPs) with the server (the Master). Together with the EEPs, agents send to the Master a scalar quantity - computed locally - that allows a full-rank Hessian approximation. The obtained approximations are averaged at the Master in order to get an approximated global Hessian, to be used to perform global NT descent steps. The approximation of the Hessian matrix at the Master is then improved by *incrementally* sending additional EEPs. In particular, for a general convex problem, SHED is designed to make use of *outdated* Hessian approximations. Thanks to this, local Hessian computation is required only sporadically. We analyze the convergence rate via the analysis of the dominant Lyapunov exponent of the objective parameter estimation error. In this novel framework, we show that the use of outdated Hessian approximations provides an improvement in the convergence rate. Furthermore, we show that the EEPs of the outdated local Hessian approximations can be shared heterogeneously with the Master, so the algorithm is versatile with respect to (per-iteration) heterogeneous CRs. We also show that, thanks to the proposed incremental strategy, SHED enjoys a super-linear convergence rate.

1.3 Organization of the paper

The rest of the paper is organized as follows: in Section 2, we detail the problem formulation and the general idea behind SHED design. In Section 3, we present SHED and the theoretical results in the linear regression (least squares) case, describing the convergence rate with respect to the algorithm parameters. Section 4 is instrumental to extending the algorithm to a general strongly convex problem, which is done later on in Section 5. At the end of Section 5, based on the theoretical results, we propose some heuristic choices for tuning SHED parameters. Finally, in Section 6, empirical performance of SHED are shown on real datasets. In particular, the theoretical results are validated and compared against

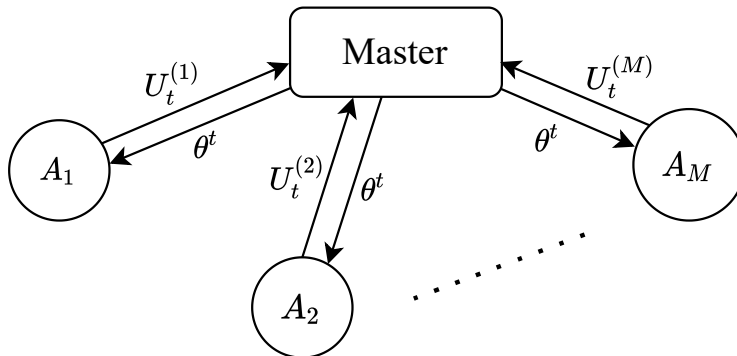


Figure 1: The typical FL optimization framework: agents A_1, \dots, A_M cooperate to solve a common learning problem. After receiving the global parameter θ^t , at the current iteration t , they share their optimization sets $U_t^{(1)}, \dots, U_t^{(M)}$ so that a new global update can be performed at the Master.

those from state-of-the-art approaches. Longer proofs and some additional experiments are reported in the Appendices, for completeness.

Notation: Vectors and matrices are written as lower and upper case bold letters, respectively (e.g., vector \mathbf{v} and matrix \mathbf{V}). The operator $\|\cdot\|$ denotes the 2-norm for vectors and the spectral norm for matrices. $\text{diag}(\mathbf{v})$ denotes a diagonal matrix with the components of vector \mathbf{v} as diagonal entries. \mathbf{I} denotes the identity matrix.

2. Problem formulation

In Fig. 1 we illustrate the typical framework of a federated learning scenario. In the rest of the paper, we denote the optimization parameter by $\theta \in \mathbb{R}^n$, and a generic cost function by $f: \mathbb{R}^n \rightarrow \mathbb{R}$, where n is the dimension of the feature data vectors $\mathbf{x} \in \mathbb{R}^n$.

Let us denote a dataset by $\mathcal{D} = \{\mathbf{x}_j, y_j\}_{j=1}^N$, where N is the global number of data samples. $\mathbf{x}_j \in \mathbb{R}^n$ denotes the j -th data sample and $y_j \in \mathbb{R}$ the response of sample j . In the case of classification problems, y_j would be an integer specifying the class to which sample \mathbf{x}_j belongs. We consider the problem of regularized empirical risk minimization of the form:

$$\min_{\theta} f(\theta), \quad (1)$$

with

$$f(\theta) := \frac{1}{N} \sum_{j=1}^N l_j(\theta) + \frac{\mu}{2} \|\theta\|_2^2,$$

where each $l_j(\theta)$ is a convex function related to the i -th element of \mathcal{D} and μ a regularization parameter. In particular,

$$l_j(\theta) = l(\mathbf{x}_j^T \theta, y_j),$$

where $l: \mathbb{R} \rightarrow \mathbb{R}$ is a convex function. Examples of convex cost functions considered in this work are:

- linear regression with quadratic cost (least squares):

$$l(\mathbf{x}_j^T \boldsymbol{\theta}, y_j) = \frac{1}{2}(\mathbf{x}_j^T \boldsymbol{\theta} - y_j)^2$$

- logistic regression:

$$l(\mathbf{x}_j^T \boldsymbol{\theta}, y_j) = \log(1 + e^{-y_j(\mathbf{x}_j^T \boldsymbol{\theta})})$$

Logistic regression belongs to the class of generalized linear models. In general, in this paper we consider optimization problems in which the following assumptions on the agents' cost functions $f^{(i)}$ hold:

Assumption 1 Let $\mathbf{H}^{(i)}(\boldsymbol{\theta}) := \nabla^2 f^{(i)}(\boldsymbol{\theta})$ the local Hessian matrix of the cost $f^{(i)}(\boldsymbol{\theta})$ of agent i . $f^{(i)}(\boldsymbol{\theta})$ is twice continuously differentiable, K_i -smooth, κ_i -strongly convex and $\mathbf{H}^{(i)}(\boldsymbol{\theta})$ is L_i -Lipschitz continuous for all $i = 1, \dots, M$.

The above assumptions imply that

$$\kappa_i \mathbf{I} \leq \mathbf{H}^{(i)}(\boldsymbol{\theta}) \leq K_i \mathbf{I}, \quad \forall \boldsymbol{\theta}$$

$$\|\mathbf{H}^{(i)}(\boldsymbol{\theta}) - \mathbf{H}^{(i)}(\boldsymbol{\theta}')\| \leq L_i \|\boldsymbol{\theta} - \boldsymbol{\theta}'\|, \quad \forall \boldsymbol{\theta}, \boldsymbol{\theta}'$$

Note that K_i -smoothness is also a consequence of the K -smoothness of any global cost function f for some constant K , while strong convexity of agents' cost functions is always guaranteed if the functions $l_j(\boldsymbol{\theta})$ are convex in the presence of a regularization term $\mu > 0$.

In the paper, we denote the data matrix by $\mathbf{X} = [\mathbf{x}_1, \dots, \mathbf{x}_N] \in \mathbb{R}^{n \times N}$, and the label vector as $\mathbf{Y} = [y_1, \dots, y_N] \in \mathbb{R}^{1 \times N}$. We refer to the dataset \mathcal{D} as the tuple $\mathcal{D} = (\mathbf{X}, \mathbf{Y})$. We denote by M the number of agents involved in the optimization algorithm, and we can write $\mathbf{X} = [\mathbf{X}_1, \dots, \mathbf{X}_M]$, $\mathbf{Y} = [\mathbf{Y}_1, \dots, \mathbf{Y}_M]$, where $\mathbf{X}_i \in \mathbb{R}^{n \times N_i}$ and $\mathbf{Y}_i \in \mathbb{R}^{1 \times N_i}$, where N_i is the number of data samples of the i -th agent. We denote the local dataset of agent i by $\mathcal{D}_i = (\mathbf{X}_i, \mathbf{Y}_i)$.

2.1 A Newton-type method based on eigendecomposition

The Newton method to solve (1) works as follows (Newton update):

$$\boldsymbol{\theta}^{t+1} = \boldsymbol{\theta}^t - \eta_t \mathbf{H}_t^{-1} \mathbf{g}_t,$$

where t denotes the t -th iteration, $\mathbf{g}_t = \mathbf{g}(\boldsymbol{\theta}_t) = \nabla f(\boldsymbol{\theta}^t)$ is the gradient at iteration t and η_t is the step size (also called learning rate) at iteration t . $\mathbf{H}_t = \nabla^2 f(\boldsymbol{\theta}^t)$ denotes the Hessian matrix at iteration t . Compared to gradient descent, the Newton method exploits the curvature information provided by the Hessian matrix to improve the descent direction. We define $\mathbf{p}_t := \mathbf{H}_t^{-1} \mathbf{g}_t$. In general, Newton-type (NT) methods try to get an approximation of \mathbf{p}_t . In an FL scenario, assuming for simplicity that all M agents have the same amount of data, we have that:

$$\mathbf{H}_t = \frac{1}{M} \sum_{i=1}^M \mathbf{H}_t^{(i)}, \quad \mathbf{g}_t = \frac{1}{M} \sum_{i=1}^M \mathbf{g}_t^{(i)}, \quad (2)$$

where $\mathbf{H}_t^{(i)} = \nabla^2 f^{(i)}(\boldsymbol{\theta}^t)$ and $\mathbf{g}_t^{(i)} = \nabla f^{(i)}(\boldsymbol{\theta}^t)$ denote local Hessian and gradient of the local cost $f^{(i)}(\boldsymbol{\theta}^t)$ of agent i , respectively. To get a Newton update at the master, in an FL setting one would need each agent to transfer the whole matrix $\mathbf{H}_t^{(i)}$ of size $O(n^2)$ to the master at each iteration, that is considered a prohibitive communication complexity in a federated learning setting, especially when the size of the feature data vectors, n , increases. Because of this, in this work we propose an algorithm in which the Newton-type update takes the form:

$$\boldsymbol{\theta}^{t+1} = \boldsymbol{\theta}^t - \eta_t \hat{\mathbf{H}}_t^{-1} \mathbf{g}_t, \quad (3)$$

where $\hat{\mathbf{H}}_t$ is an approximation of \mathbf{H}_t . In some previous contributions, like Wang et al. (2018); T. Dinh et al. (2022), $\hat{\mathbf{H}}_t$ is the harmonic mean of local Hessians, obtained at the master through an intermediate additional communication round to provide each agent with the global gradient \mathbf{g}_t . In the recent FedNL algorithm (Safaryan et al., 2021), each agent at each iteration sends a compressed version of a Hessian-related matrix. In the best performing version of the algorithm, the rank-1 approximation using the first eigenvector of the matrix is sent. Authors show that thanks to this procedure they can eventually get the Hessian matrix at the optimum, which provides super-linear convergence rate.

Instead, our proposal is to incrementally obtain at the master an average of full-rank approximations of local Hessians through the communication of the local Hessian most relevant eigenvectors together with a carefully computed local approximation parameter. In particular, we approximate the Hessian matrix \mathbf{H}_t exploiting eigendecomposition in the following way: the symmetric positive definite Hessian \mathbf{H}_t can be diagonalized as $\mathbf{H}_t = \mathbf{V}_t \boldsymbol{\Lambda}_t \mathbf{V}_t^T$, with $\boldsymbol{\Lambda}_t = \text{diag}(\lambda_{1,t}, \dots, \lambda_{n,t})$, where $\lambda_{k,t}$ is the eigenvalue corresponding to the k -th eigenvector, $\mathbf{v}_{k,t}$. \mathbf{H}_t can be approximated as

$$\hat{\mathbf{H}}_t := \hat{\mathbf{H}}_t(\rho_t, q_t) = \mathbf{V}_t \hat{\boldsymbol{\Lambda}}_t \mathbf{V}_t^T = \sum_{k=1}^{q_t} (\lambda_{k,t} - \rho_t) \mathbf{v}_{k,t} \mathbf{v}_{k,t}^T + \rho_t \mathbf{I}, \quad (4)$$

with $\hat{\boldsymbol{\Lambda}}_t := \hat{\boldsymbol{\Lambda}}_t(\rho_t, q_t) = \text{diag}(\lambda_{1,t}, \dots, \lambda_{q_t,t}, \rho_t, \dots, \rho_t)$. The scalar $\rho_t > 0$ is the approximation parameter (if $\rho_t = 0$ this becomes a low-rank approximation). The integer $q_t = 1, \dots, n$ denotes the number of eigenvalue-eigenvector pairs (EEPs) $\{\lambda_{k,t}, \mathbf{v}_{k,t}\}_{k=1}^{q_t}$ being used to approximate the Hessian matrix. We always consider eigenvalues ordered so that $\lambda_{1,t} \geq \lambda_{2,t} \geq \dots \geq \lambda_{n,t}$. The approximation of Eqn. (4) was used in Erdogdu and Montanari (2015) for a subsampled centralized optimization problem. There, the parameter ρ_t was chosen to be equal to λ_{q_t+1} . In the FL setting, we use approximation shown in Eqn. (4) to approximate the local Hessian matrices of the agents. In particular, letting $\hat{\mathbf{H}}_t^{(i)}$ be the approximated local Hessian of agent i , the approximated global Hessian is the average of the local approximated Hessian matrices:

$$\hat{\mathbf{H}}_t = \sum_{i=1}^M p_i \hat{\mathbf{H}}_t^{(i)}, \quad p_i = N_i/N$$

where $\hat{\mathbf{H}}_t^{(i)} := \hat{\mathbf{H}}_t(\rho_t^{(i)}, q_t^{(i)})$ is a function of the local approximation parameter $\rho_t^{(i)}$ and of the number of eigenvalue-eigenvector pairs $q_t^{(i)}$ shared by agent i , which are denoted by $\{\lambda_{k,t}^{(i)}, \mathbf{v}_{k,t}^{(i)}\}_{k=1}^{q_t^{(i)}}$.

2.2 The algorithm in a nutshell

The idea of the SHED algorithm is that agents share with the Master, together with the gradient, some of their local Hessian EEPs, according to the available CRs. They share the EEPs in a decreasing order dictated by the value of the positive eigenvalues corresponding to the eigenvectors. At each iteration, they incrementally add new EEPs to the information they have sent to the Master. In a linear regression problem, in which the Hessian does not depend on the current parameter, agents would share their EEPs incrementally up to the n -th. When the n -th EEP is shared, the Master has the full Hessian available and no further second order information needs to be transmitted. In a general convex problem, in which the Hessian matrix changes at each iteration, as it is a function of the current parameter, SHED is designed in a way in which agents perform a *renewal* operation at certain iterations, i.e., they re-compute the Hessian matrix and re-start sharing the EEPs from the most relevant ones of the new matrix.

3. Linear regression (least squares)

In this section we illustrate our algorithm and present the convergence analysis considering the problem of solving (1) via Newton-type updates (3) in the least squares (LSs) case, i.e., in the case of linear regression with quadratic cost. Before moving to the FL case, we prove some results for the convergence rate of the centralized iterative least squares problem.

First, we provide some important definitions. In the case of linear regression with quadratic cost, the Hessian is such that $\mathbf{H}_{LS} := \mathbf{H}(\boldsymbol{\theta})$, $\forall \boldsymbol{\theta}$, i.e., the Hessian does not depend on the parameter $\boldsymbol{\theta}$. Because of this, when considering LSs, we write the eigendecomposition as $\mathbf{H}_{LS} = \mathbf{V}\boldsymbol{\Lambda}\mathbf{V}^T$, with $\boldsymbol{\Lambda} = \text{diag}(\lambda_1, \dots, \lambda_n)$ without specifying the iteration t when not needed. Let $\boldsymbol{\theta}^*$ denote the solution to (1). In the following, we use the fact that the cost for parameter $\boldsymbol{\theta}^t$ can be written as $f(\boldsymbol{\theta}^t) = f(\boldsymbol{\theta}^*) + \bar{f}(\boldsymbol{\theta}^t)$, with $\bar{f}(\boldsymbol{\theta}^t) := \frac{1}{2}(\boldsymbol{\theta}^t - \boldsymbol{\theta}^*)^T \mathbf{H}_{LS}(\boldsymbol{\theta}^t - \boldsymbol{\theta}^*)$. Similarly, the gradient can be written as $\mathbf{g}_t = \mathbf{H}_{LS}(\boldsymbol{\theta}^t - \boldsymbol{\theta}^*)$.

In this setup, the update rule of Eqn. (3) can be written as a time-varying linear discrete-time system:

$$\boldsymbol{\theta}^{t+1} - \boldsymbol{\theta}^* = \mathbf{A}_t(\boldsymbol{\theta}^t - \boldsymbol{\theta}^*) \quad (5)$$

where

$$\mathbf{A}_t := \mathbf{A}(\rho_t, \eta_t, q_t) = \mathbf{I} - \eta_t \hat{\mathbf{H}}_t^{-1} \mathbf{H}_{LS}.$$

Indeed,

$$\begin{aligned} \boldsymbol{\theta}^{t+1} - \boldsymbol{\theta}^* &= \boldsymbol{\theta}^t - \boldsymbol{\theta}^* - \eta_t \hat{\mathbf{H}}_t^{-1} \mathbf{g}_t \\ &= \boldsymbol{\theta}^t - \boldsymbol{\theta}^* - \eta_t \hat{\mathbf{H}}_t^{-1} \mathbf{H}_{LS}(\boldsymbol{\theta}^t - \boldsymbol{\theta}^*) \\ &= (\mathbf{I} - \eta_t \hat{\mathbf{H}}_t^{-1} \mathbf{H}_{LS})(\boldsymbol{\theta}^t - \boldsymbol{\theta}^*). \end{aligned}$$

3.1 Centralized iterative least squares

In this sub-section, we study the optimization problem in the centralized case, so when all the data is kept in a single machine. We provide a range of choices for the approximation parameter ρ_t that are optimal in the convergence rate sense. We denote the convergence factor of the descent algorithm described by Eqn. (3) by

$$r_t := r(\rho_t, \eta_t, q_t),$$

making its dependence on the tuple (ρ_t, η_t, q_t) explicit.

Theorem 1 *Consider solving problem (1) via Newton-type updates (3) in the least squares case. At iteration t , let the Hessian matrix \mathbf{H}_{LS} be approximated as in Eqn. (4) (centralized case). The convergence rate is described by*

$$\|\boldsymbol{\theta}^{t+1} - \boldsymbol{\theta}^*\| \leq r_t \|\boldsymbol{\theta}^t - \boldsymbol{\theta}^*\|. \quad (6)$$

For a given $q_t \in \{0, 1, \dots, n\}$ the best achievable convergence factor is

$$r_t^* = r^*(q_t) := \min_{(\rho_t, \eta_t)} r(\rho_t, \eta_t, q_t) = \left(1 - \frac{\lambda_n}{\rho_t^*}\right), \quad (7)$$

where

$$\rho_t^* := (\lambda_{q_t+1} + \lambda_n)/2. \quad (8)$$

r_t^* is achievable if and only if $(\rho_t, \eta_t) \in \mathcal{S}^*$, with

$$\mathcal{S}^* = \left\{ (\rho_t, \eta_t) : \rho_t \in [\lambda_n, \lambda_{q_t+1}], \eta_t^* = \frac{2\rho_t}{\lambda_{q_t+1} + \lambda_n} \right\} \quad (9)$$

Proof From (4), writing $\mathbf{H}_{LS} = \mathbf{V}\boldsymbol{\Lambda}\mathbf{V}^T$ and $\hat{\mathbf{H}}_t = \mathbf{V}\hat{\boldsymbol{\Lambda}}_t\mathbf{V}^T$, with $\hat{\boldsymbol{\Lambda}}_t = \text{diag}(\lambda_1, \dots, \lambda_{q_t}, \rho_t, \dots, \rho_t)$, define $\boldsymbol{\theta}_{\rho_t, \eta_t}^{t+1} := \boldsymbol{\theta}^t - \eta_t \hat{\mathbf{H}}_t^{-1} \mathbf{g}_t$. Recalling that $\mathbf{g}_t = \mathbf{H}_{LS}(\boldsymbol{\theta}^t - \boldsymbol{\theta}^*)$, we have:

$$\begin{aligned} \boldsymbol{\theta}_{\rho_t, \eta_t}^{t+1} - \boldsymbol{\theta}^* &= \mathbf{A}_t(\boldsymbol{\theta}^t - \boldsymbol{\theta}^*) = (\mathbf{I} - \eta_t \hat{\mathbf{H}}_t^{-1} \mathbf{H}_{LS})(\boldsymbol{\theta}^t - \boldsymbol{\theta}^*) \\ &= \mathbf{V}(\mathbf{I} - \eta_t \hat{\boldsymbol{\Lambda}}_t^{-1} \boldsymbol{\Lambda})\mathbf{V}^T(\boldsymbol{\theta}^t - \boldsymbol{\theta}^*). \end{aligned} \quad (10)$$

For some given $q_t \in \{1, \dots, n\}$, r_t is a function of two tunable parameters, i.e., the tuple (η_t, ρ_t) . We now prove that r_t^* can be achieved if and only if $\rho_t \in [\lambda_n, \lambda_{q_t+1}]$. The convergence rate is determined by the eigenvalue of $(\mathbf{I} - \eta_t \hat{\boldsymbol{\Lambda}}_t^{-1} \boldsymbol{\Lambda})$ with the greatest absolute value. First, we show that $\rho_t \notin [\lambda_n, \lambda_{q_t+1}]$ implies $r_t > r_t^*$, then we show that, if $\rho_t \in [\lambda_n, \lambda_{q_t+1}]$, there exists an optimal η_t^* for which r_t^* is achieved. If $\rho_t < \lambda_n$, the choice of η_t minimizing the maximum absolute value of $(\mathbf{I} - \eta_t \hat{\boldsymbol{\Lambda}}_t^{-1} \boldsymbol{\Lambda})$ is the solution of $|1 - \eta_t| = |1 - \eta_t \lambda_{q_t+1}/\rho_t|$, which is $\eta_t^* = 2\rho_t/(\rho_t + \lambda_{q_t+1})$. The corresponding convergence factor is $1 - \eta_t^* > r_t^*$. Similarly, if $\rho_t > \lambda_{q_t+1}$, one gets $\eta_t^* = 2\rho_t/(\rho_t + \lambda_n)$ and convergence factor equal to $1 - 2\lambda_n/(\rho_t + \lambda_n) > r_t^*$. If $\rho_t \in [\lambda_n, \lambda_{q_t+1}]$, the best η_t is such that $|1 - \eta_t \lambda_n/\rho_t| = |1 - \eta_t \lambda_{q_t+1}/\rho_t|$, whose solution is

$$\eta_t^* = \frac{2\rho_t}{\lambda_{q_t+1} + \lambda_n} \quad (11)$$

and the achieved factor is $r_t = 1 - \eta_t^* \lambda_n/\rho_t = 1 - \lambda_n/\rho_t^* = r_t^*$. We see that the definition of the set \mathcal{S}^* immediately follows. \blacksquare

In the above Theorem, we have shown that the best convergence rate is achievable, by tuning the step size, as long as $\rho_t \in [\lambda_n, \lambda_{q_t+1}]$. In the following Corollary, we provide an optimal choice for the tuple (ρ_t, η_t) with respect to the estimation error.

Corollary 2 *Among the tuples $(\rho_t, \eta_t) \in \mathcal{S}^*$, the choice of the tuple $(\rho_t^*, 1)$, with ρ_t^* defined in (8), is optimal with respect to the estimation error $\|\boldsymbol{\theta}_{\rho_t, \eta_t}^{t+1} - \boldsymbol{\theta}^*\|$, for any $\boldsymbol{\theta}^t$ and for any t , in the sense that*

$$\|\boldsymbol{\theta}_{\rho_t^*, 1}^{t+1} - \boldsymbol{\theta}^*\| \leq \|\boldsymbol{\theta}_{\rho_t, \eta_t}^{t+1} - \boldsymbol{\theta}^*\|, \quad \forall (\eta_t, \rho_t) \in \mathcal{S}^*$$

Proof Define $\mathbf{B}_t^* := (\mathbf{I} - (\hat{\Lambda}_t(\rho_t^*, q_t))^{-1} \mathbf{A}) = \text{diag}(0, \dots, 0, 1 - \lambda_{q_t+1}/\rho_t^*, \dots, 1 - \lambda_n/\rho_t^*)$. For $\rho_t \neq \rho_t^*$, with $\rho_t \in [\lambda_n, \lambda_{q_t+1}]$, define $\mathbf{B}_t := (\mathbf{I} - \eta_t^* (\hat{\Lambda}_t(\rho_t, q_t))^{-1} \mathbf{A}) = \text{diag}(1 - \eta_t^*, \dots, 1 - \eta_t^*, 1 - \lambda_{q_t+1}/\rho_t^*, \dots, 1 - \lambda_n/\rho_t^*) = \mathbf{B}_t^* + \delta \mathbf{B}_t$, with $\delta \mathbf{B}_t = \text{diag}(1 - \eta_t^*, \dots, 1 - \eta_t^*, 0, \dots, 0)$, where η_t^* is defined in (11) and ρ_t^* in (8). Now define $\mathbf{z}^t := \mathbf{V}^T(\boldsymbol{\theta}^t - \boldsymbol{\theta}^*)$ and $\mathbf{z}_{\rho_t, \eta_t}^{t+1} := \mathbf{V}^T(\boldsymbol{\theta}_{\rho_t, \eta_t}^{t+1} - \boldsymbol{\theta}^*)$, where $(\boldsymbol{\theta}_{\rho_t, \eta_t}^{t+1} - \boldsymbol{\theta}^*)$ is defined in (10). We have

$$\|\boldsymbol{\theta}_{\rho_t^*, 1}^{t+1} - \boldsymbol{\theta}^*\|^2 = \|\mathbf{z}_{\rho_t^*, 1}^{t+1}\|^2 = \|\mathbf{B}_t^* \mathbf{z}^t\|^2,$$

$$\|\boldsymbol{\theta}_{\rho_t, \eta_t}^{t+1} - \boldsymbol{\theta}^*\|^2 = \|\mathbf{B}_t \mathbf{z}^t\|^2 = \|\mathbf{B}_t^* \mathbf{z}^t\|^2 + \|\delta \mathbf{B}_t \mathbf{z}^t\|^2,$$

because the cross term is $2(\mathbf{B}_t^* \mathbf{z}^t)^T (\delta \mathbf{B}_t \mathbf{z}^t) = 0$. We see that, for any t and for any $\boldsymbol{\theta}^t$,

$$\|\boldsymbol{\theta}_{\rho_t^*, 1}^{t+1} - \boldsymbol{\theta}^*\| \leq \|\boldsymbol{\theta}_{\rho_t, \eta_t}^{t+1} - \boldsymbol{\theta}^*\|$$

■

We remark that the bound in (6) is tight for $r_t = r_t^*$. If q_t increases, the convergence factor r_t^* decreases until it becomes zero, when $q_t = n - 1$, thus we can have convergence in a finite number of steps.

3.2 Federated least squares

We now consider the FL scenario described in section 2, in which M agents keep their local data and share optimization parameters to contribute to the learning algorithm.

Assumption 2 *In the rest of the paper, we assume that each agent has the same amount of data samples, $N_i = \frac{N}{M}$. This allows us to express global functions, such as the gradient, as the arithmetic mean of local functions (e.g., $\mathbf{g}_t = (1/M) \sum_{i=1}^M \mathbf{g}_t^{(i)}$).*

This assumption is made only for notation convenience. It is straightforward to show that all the results are valid also for N_i different for each i . To show it, it is sufficient to replace the arithmetic mean of local functions with the weighted average, weighting each local function with $p_i = N_i/N$. As an example, the global gradient would be written in the following way:

$$\mathbf{g}_t = \sum_{i=1}^M p_i \mathbf{g}_t^{(i)}, \quad p_i = N_i/N$$

In this subsection we introduce the algorithm for the LSs case (Algorithm 1), that is a special case of Algorithm 4, described in Sec. 5, which is designed for a general convex cost. We refer to Algorithm 1 as SHED-LS and it works as follows: at iteration t , each

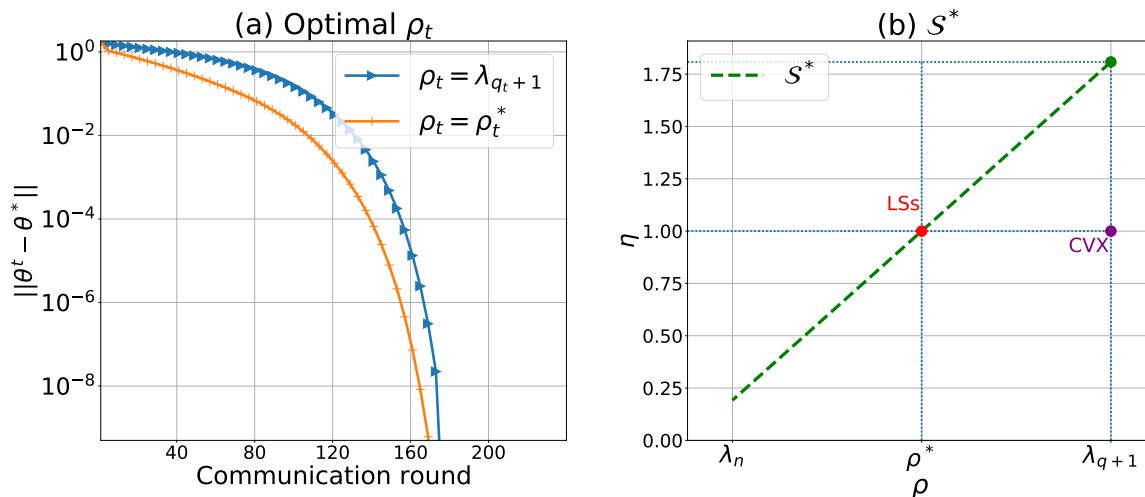


Figure 2: Performance comparison for different values of ρ_t . The best choice in terms of estimation error from Corollary 2 is compared against the choice that was proposed in Erdogdu and Montanari (2015), that is $\rho_t = \lambda_{q_t+1}$. In (b), we show an example of the set \mathcal{S}^* , and outline two points: LSs in red is the choice of the tuple in \mathcal{S}^* providing the optimal convergence factor in LSs, while the purple CVX which does not belong to \mathcal{S}^* , and it is the choice which we do in the scenario of FL with convex cost

device shares with the Master some of its local Hessian eigenvectors scaled by quantities related to the corresponding eigenvalues. The eigenvectors are shared *incrementally*, where the order in which they are shared is given by the corresponding eigenvalues. For example, at $t = 1$ agent i will start by sharing its first Hessian eigenvectors $\mathbf{v}_1^{(i)}, \dots, \mathbf{v}_{q_1}^{(i)}$ according to its communication resources (CRs) and then will incrementally send up to $\mathbf{v}_{n-1}^{(i)}$ in the following iterations. To enable the approximation of the local Hessian via a limited number of eigenvectors using (4), each eigenvector is sent to the Master together with $\lambda_j^{(i)}$ and the parameter $\rho_t^{(i)}$. The Master averages the received information to obtain an estimate of the global Hessian as follows:

$$\hat{\mathbf{H}}_t = \frac{1}{M} \sum_{i=1}^M \hat{\mathbf{H}}_t^{(i)}, \quad (12)$$

where $\hat{\mathbf{H}}_t^{(i)}$ is

$$\hat{\mathbf{H}}_t^{(i)} := \hat{\mathbf{H}}^{(i)}(\rho_t^{(i)}, q_t^{(i)}) = \sum_{j=1}^{q_t^{(i)}} (\lambda_j^{(i)} - \rho_t^{(i)}) \mathbf{v}_j^{(i)} \mathbf{v}_j^{(i)T} + \rho_t^{(i)} \mathbf{I}, \quad (13)$$

in which $q_t^{(i)}$ is the number of the local Hessian eigenvectors-eigenvalues pairs that agent i has already sent to the Master at iteration t . We denote by $d_t^{(i)}$ the *increment*, meaning

Algorithm 1: Federated Least Squares - SHED-LS

Input: $\{\mathcal{D}_i\}_{i=1}^M = \{(\mathbf{X}_i, \mathbf{Y}_i)\}_{i=1}^M$, t_{max} , $\boldsymbol{\theta}^0$, $\mathcal{A} = \{\text{agents}\}$, $\mathcal{I} = \{1\}$
Output: $\boldsymbol{\theta}^{t_{max}}$

```

1 for  $t \leftarrow 1$  to  $t_{max}$  do
2   for agent  $i \in \mathcal{A}$  do
3     when Received  $\boldsymbol{\theta}^t$  from the Master do
4       if  $t \in \mathcal{I}$  then
5         compute  $\mathbf{H}_{LS}^{(i)} = \nabla^2 f^{(i)}(\boldsymbol{\theta}^t) = \mathbf{X}_i \mathbf{X}_i^T$ 
6          $\{(\lambda_j^{(i)}, \mathbf{v}_j^{(i)})\}_{j=1}^n \leftarrow \text{eigendec}(\mathbf{H}_{LS}^{(i)})$  // eigendecomposition
7          $q_0^{(i)} \leftarrow 0$ 
8         compute  $\mathbf{g}_t^{(i)} = \nabla f^{(i)}(\boldsymbol{\theta}^t)$ 
9         set  $d_t^{(i)}$  // according to CRs
10         $q_t^{(i)} \leftarrow q_{t-1}^{(i)} + d_t^{(i)}$  // increment
11         $\rho_t^{(i)} \leftarrow (\lambda_{q_t^{(i)}+1}^{(i)} + \lambda_n^{(i)})/2$  // approximation parameter
12         $U_t^{(i)} \leftarrow \{ \{\mathbf{v}_j^{(i)}, \lambda_j^{(i)}\}_{j=q_{t-1}^{(i)}+1}^{q_t^{(i)}}, \mathbf{g}_t^{(i)}, \rho_t^{(i)} \}$ 
13        Send  $U_t^{(i)}$  to the Master.
14
15 At the Master:
16 when Received  $U_t^{(i)}$  from all agents do
17   compute  $\hat{\mathbf{H}}_t^{(i)}, \forall i.$  // see (13)
18   Compute  $\hat{\mathbf{H}}_t$  (as in eq. (12)) and  $\mathbf{g}_t$ .
19   Perform Newton-type update (3) with  $\eta_t = 1$ .
20   Broadcast  $\boldsymbol{\theta}^{t+1}$  to all agents.
    
```

the number of eigenvectors that agent i can send to the Master at iteration t . Given the results shown in Section 3.1, in this Section we fix the local approximation parameter to be $\rho_t^{(i)} = \rho_t^{(i)*} = (\lambda_{q_t^{(i)}+1}^{(i)} + \lambda_n^{(i)})/2$ and the step size to be $\eta_t = 1$. The following results related to the convergence rate allow the value $q_t^{(i)}$ to be different for each agent i , so we define

$$\mathbf{q}_t = [q_t^{(1)}, \dots, q_t^{(M)}]^T, \quad q_t^{(i)} \in \{0, \dots, n\} \quad \forall i \in \{1, \dots, M\}$$

By construction, the matrix $\hat{\mathbf{H}}_t$ is positive definite, being the sum of positive definite matrices, implying that $-\mathbf{p}_t = -\hat{\mathbf{H}}_t^{-1} \mathbf{g}_t$ is a descent direction.

Theorem 3 Consider the problem in (1) in the least squares case. Given $\hat{\mathbf{H}}_t$ defined in (12), the update rule defined in (3) is such that, for $\rho_t^{(i)} = (\lambda_{q_t^{(i)}+1}^{(i)} + \lambda_n^{(i)})/2$ and $\eta_t = 1$:

$$\|\boldsymbol{\theta}^{t+1} - \boldsymbol{\theta}^*\| \leq c_t \|\boldsymbol{\theta}^t - \boldsymbol{\theta}^*\|, \quad (14)$$

with $c_t = (1 - \bar{\lambda}_n/\bar{\rho}_t)$ and

$$\bar{\rho}_t := \bar{\rho}(\mathbf{q}_t) = \frac{1}{M} \sum_{i=1}^M \rho_t^{(i)}, \quad \bar{\lambda}_n = \frac{1}{M} \sum_{i=1}^M \lambda_n^{(i)}. \quad (15)$$

If Algorithm 1 is applied, $c_{t+1} \leq c_t \forall t$, and, if for all i it holds that $q_t^{(i)} = n - 1$, at some iteration t' $c_{t'} = 0$.

Proof Fix $\eta_t = 1$ in (5),

$$\boldsymbol{\theta}^{t+1} - \boldsymbol{\theta}^* = \mathbf{A}_t(\boldsymbol{\theta}^t - \boldsymbol{\theta}^*) = (\mathbf{I} - \hat{\mathbf{H}}_t^{-1} \mathbf{H}_{LS})(\boldsymbol{\theta}^t - \boldsymbol{\theta}^*).$$

We have that

$$\begin{aligned} \|\boldsymbol{\theta}^{t+1} - \boldsymbol{\theta}^*\| &\leq \|\mathbf{I} - \hat{\mathbf{H}}_t^{-1} \mathbf{H}_{LS}\| \|\boldsymbol{\theta}^t - \boldsymbol{\theta}^*\| \\ &\leq \|\hat{\mathbf{H}}_t^{-1}\| \|\hat{\mathbf{H}}_t - \mathbf{H}_{LS}\| \|\boldsymbol{\theta}^t - \boldsymbol{\theta}^*\| \\ &\leq \frac{(\bar{\rho}_t - \bar{\lambda}_n)}{\bar{\rho}_t} \|\boldsymbol{\theta}^t - \boldsymbol{\theta}^*\| \end{aligned}$$

The last inequality follows from two inequalities: (i) $\|\hat{\mathbf{H}}_t^{-1}\| \leq 1/\bar{\rho}_t$ and (ii) $\|\hat{\mathbf{H}}_t - \mathbf{H}_{LS}\| \leq \bar{\rho}_t - \bar{\lambda}_n$.

(i) holds because $\|\hat{\mathbf{H}}_t^{-1}\| = (\lambda_{\min}(\hat{\mathbf{H}}_t))^{-1}$, and $\lambda_{\min}(\hat{\mathbf{H}}_t) \geq \bar{\rho}_t$, thus implying $\|\hat{\mathbf{H}}_t^{-1}\| \leq 1/\bar{\rho}_t$.

(ii) follows recalling that $\mathbf{H}_{LS} = \frac{1}{M} \sum_{i=1}^M \mathbf{H}_{LS}^{(i)}$, with $\mathbf{H}_{LS}^{(i)}$ the local Hessian at agent i . We have

$$\|\hat{\mathbf{H}}_t - \mathbf{H}_{LS}\| = \frac{1}{M} \left\| \sum_{i=1}^M (\hat{\mathbf{H}}_t^{(i)} - \mathbf{H}_{LS}^{(i)}) \right\| \leq \frac{1}{M} \sum_{i=1}^M \|\hat{\mathbf{H}}_t^{(i)} - \mathbf{H}_{LS}^{(i)}\|.$$

Being $\hat{\mathbf{H}}_t^{(i)} - \mathbf{H}_{LS}^{(i)}$ symmetric, it holds that

$$\|\hat{\mathbf{H}}_t^{(i)} - \mathbf{H}_{LS}^{(i)}\| = \max_j |\lambda_j(\hat{\mathbf{H}}_t^{(i)} - \mathbf{H}_{LS}^{(i)})| = \rho_t^{(i)} - \lambda_n^{(i)},$$

where the last equality holds because

$$\hat{\mathbf{H}}_t^{(i)} - \mathbf{H}_{LS}^{(i)} = \mathbf{V}^{(i)} (\hat{\boldsymbol{\Lambda}}_t^{(i)} - \boldsymbol{\Lambda}_t^{(i)}) \mathbf{V}^{(i)T} \quad (16)$$

where

$$\begin{aligned} \hat{\boldsymbol{\Lambda}}_t^{(i)} &= \text{diag}(\lambda_1^{(i)}, \dots, \lambda_{q_t^{(i)}}^{(i)}, \rho_t^{(i)}, \dots, \rho_t^{(i)}), \\ \boldsymbol{\Lambda}_t^{(i)} &= \text{diag}(\lambda_1^{(i)}, \dots, \lambda_{q_t^{(i)}}^{(i)}, \lambda_{q_t^{(i)}+1}^{(i)}, \dots, \lambda_n^{(i)}), \end{aligned} \quad (17)$$

and because $\rho_t^{(i)} = (\lambda_{q_t^{(i)}+1}^{(i)} + \lambda_n^{(i)})/2$. ■

This theorem shows that our approach in the LSs case provides convergence in a finite number of iterations, if $q_t^{(i)}$ keeps increasing through time for each agent i . Indeed, as in the centralized case, if $q_t^{(i)}$ increases for all i , the factor c_t decreases until it becomes zero. Furthermore, each agent is free to send at each iterations an arbitrary number of eigenvector-eigenvalue pairs, according to its CRs, and by doing so it can improve the convergence rate.

4. From least squares to strongly convex cost

We want to extend the analysis and algorithm presented in the previous sections of the paper to a general convex cost $f(\boldsymbol{\theta}^t)$. With respect to the proposed approach, the general convex case requires special attention for two main reasons: (i) the update rule defined in (3) requires tuning of the step-size η_t , usually via backtracking line search, and (ii) the Hessian matrix is in general a function of the parameter $\boldsymbol{\theta}$. In this section, still focusing on the least squares case, we provide some results that are instrumental to the analysis of the general convex case.

4.1 Backtracking line search for step size tuning

We recall the well-known Armijo-Goldstein condition for accepting a step size η_t via backtracking line search:

$$f(\boldsymbol{\theta}^t - \eta_t \mathbf{p}) \leq f(\boldsymbol{\theta}^t) - \alpha \eta_t \mathbf{p}^T \mathbf{g}_t, \quad (18)$$

where $\alpha \in (0, 1/2)$. The corresponding line search algorithm is the following:

Algorithm 2: Backtracking line search algorithm

Input: $\alpha \in (0, 1/2)$, $\beta \in (0, 1)$, $\boldsymbol{\theta}^t$, \mathbf{p}_t , \mathbf{g}_t , f
Output: $\bar{\eta}_t$

- 1 $\eta_t^0 \leftarrow 1$, $k \leftarrow 0$
- 2 **while** $f(\boldsymbol{\theta}^t - \eta_t^{(k)} \mathbf{p}) > f(\boldsymbol{\theta}^t) - \alpha \eta_t^{(k)} \mathbf{p}^T \mathbf{g}_t$ **do**
- 3 $k \leftarrow k + 1$
- 4 $\eta_t^{(k)} = \beta \eta_t^{(k-1)}$
- 5 $\bar{\eta}_t = \eta_t^{(k)}$

Lemma 4 Consider the problem in (1) in the least squares case. Let $\mathbf{p}_t = \hat{\mathbf{H}}_t^{-1} \mathbf{g}_t$, with $\hat{\mathbf{H}}_t$ defined in (12). A sufficient condition for a step size η_t to satisfy Armijo-Goldstein condition (18), for any $\alpha \in (0, 1/2)$, is

$$\eta_t = \min_{i=1, \dots, M} \frac{\rho_t^{(i)}}{\lambda_{q_t^{(i)}+1}^{(i)}} \quad (19)$$

Proof The quadratic cost in $\boldsymbol{\theta}^t$ can be written as

$$f(\boldsymbol{\theta}^t) = f(\boldsymbol{\theta}^*) + \bar{f}(\boldsymbol{\theta}^t).$$

with $\bar{f}(\boldsymbol{\theta}^t) = \frac{1}{2}(\boldsymbol{\theta}^t - \boldsymbol{\theta}^*)^T \mathbf{H}_{LS}(\boldsymbol{\theta}^t - \boldsymbol{\theta}^*)$. Given that $f(\boldsymbol{\theta}^*)$ does not depend on $\boldsymbol{\theta}^t$, we can focus on $\bar{f}(\boldsymbol{\theta}^t)$.

We have that

$$\begin{aligned} \bar{f}(\boldsymbol{\theta}^t - \eta_t \mathbf{p}_t) &= \frac{1}{2}(\boldsymbol{\theta}^t - \eta_t \mathbf{p}_t - \boldsymbol{\theta}^*)^T \mathbf{H}_{LS}(\boldsymbol{\theta}^t - \eta_t \mathbf{p}_t - \boldsymbol{\theta}^*) \\ &\stackrel{(1)}{=} \bar{f}(\boldsymbol{\theta}^t) + \frac{1}{2} \eta_t^2 \mathbf{p}_t^T \mathbf{H}_{LS} \mathbf{p}_t - \eta_t \mathbf{p}_t^T \mathbf{g}_t \\ &\stackrel{(2)}{=} \bar{f}(\boldsymbol{\theta}^t) - \eta_t \mathbf{p}_t^T (\hat{\mathbf{H}}_t - \eta_t \frac{\mathbf{H}_{LS}}{2}) \mathbf{p}_t \end{aligned} \quad (20)$$

where we have used identity $\mathbf{H}_{LS}(\boldsymbol{\theta}_t - \boldsymbol{\theta}^*) = \mathbf{g}_t$ and the fact that $\mathbf{p}_t^T \mathbf{g}_t = \mathbf{p}_t^T \hat{\mathbf{H}}_t \hat{\mathbf{H}}_t^{-1} \mathbf{g}_t = \mathbf{p}_t^T \hat{\mathbf{H}}_t \mathbf{p}_t$ to get equality (1) and (2), respectively. We see that if

$$\hat{\mathbf{H}}_t - \eta_t \mathbf{H}_{LS}/2 \geq \hat{\mathbf{H}}_t/2, \quad (21)$$

then Armijo-Goldstein condition (18) is satisfied. Indeed, in that case,

$$\begin{aligned} \bar{f}(\boldsymbol{\theta}^t) - \eta_t \mathbf{p}_t^T (\hat{\mathbf{H}}_t - \eta_t \frac{\mathbf{H}_{LS}}{2}) \mathbf{p}_t &\leq \bar{f}(\boldsymbol{\theta}^t) - \frac{1}{2} \eta_t \mathbf{p}_t^T \hat{\mathbf{H}}_t \mathbf{p}_t \\ &\leq \bar{f}(\boldsymbol{\theta}^t) - \alpha \eta_t \mathbf{p}_t^T \mathbf{g}_t. \end{aligned}$$

So, we need to find a sufficient condition on η_t for (21) to be true. We see that (21) is equivalent to $\hat{\mathbf{H}}_t - \eta_t \mathbf{H}_{LS} \geq 0$. We have $\hat{\mathbf{H}}_t - \eta_t \mathbf{H}_{LS} = \frac{1}{M} \sum_{i=1}^M \mathbf{V}^{(i)} (\hat{\Lambda}_t^{(i)} - \eta_t \Lambda_t^{(i)}) \mathbf{V}^{(i)T}$, and, $\forall i$, all the elements of the diagonal matrix $\hat{\Lambda}_t^{(i)} - \eta_t \Lambda_t^{(i)}$ are positive if $\eta_t \leq \rho_t^{(i)} / \lambda_{q_t^{(i)}+1}^{(i)}$ (see Eq. (17)), and we see that the choice (19) provides a sufficient condition to satisfy (21), from which we can conclude. \blacksquare

Corollary 5 *In the least squares case (Algorithm 1), choosing $\rho_t^{(i)} = \rho_t^{(i)*}$, $\forall i$, Armijo backtracking line search (Algorithm 2) would choose a step size $\eta_t \geq \frac{1}{2}$. Choosing $\rho_t^{(i)} = \lambda_{q_t^{(i)}+1}^{(i)}$, $\forall i$, Armijo backtracking line search would choose a step size $\eta_t = 1$.*

Proof The proof is straightforward from Eqn. (19) of Lemma 4. \blacksquare

Remark 6 *For the choice $\rho^{(i)} = \rho^{(i)*}$, the Armijo-backtracking might not choose a step size $\eta_t = 1$ even for arbitrarily small $\alpha < 0.5$. Indeed, we can easily build a counter-example in the centralized case considering $\hat{\mathbf{H}}_t = \hat{\Lambda}_t = \text{diag}(\lambda_1, \dots, \lambda_q, \rho^*, \dots, \rho^*)$, a gradient \mathbf{g}_t such that $\mathbf{p}_t = \hat{\mathbf{H}}_t^{-1} \mathbf{g}_t = [0, \dots, 0, 1, 0, \dots, 0]^T$ (e.g., $\mathbf{g}_t = [0, \dots, 0, \lambda_{q+1}, 0, \dots, 0]^T$). We see that with $\eta_t = 1$, Eq. (20) becomes $f(\boldsymbol{\theta}^{t+1}) = f(\boldsymbol{\theta}^t) - \lambda_n/2$ and, in order to be satisfied, the Armijo condition would require $\alpha \leq \frac{\lambda_n}{\lambda_{q+1} + \lambda_n}$, where the right hand side can become arbitrarily small depending on the eigenspectrum.*

The results of Lemma 4 and of Corollary 5 and the counter-example of the above Remark are important for the design of the algorithm in the general convex case. Indeed, as illustrated in the next Section (Section 5), a requirement for the theoretical results on the convergence rate is that the step size becomes equal to one, which is not guaranteed by the Armijo backtracking line search, even when considering the least squares case, if $\rho_t^{(i)} < \lambda_{q_t^{(i)}+1}^{(i)}$. For this reason, the algorithm in the general convex case is designed with $\rho_t^{(i)} = \lambda_{q_t^{(i)}+1}^{(i)}$

4.2 Algorithm with periodic renewals

Now, we introduce a variant of Algorithm 1 that is instrumental to study the convergence rate of the proposed algorithm in the general convex case. The variant is Algorithm 3. The definition of $\mathcal{I} = \{1, T, 2T, \dots\}$ implies that every T iterations the incremental strategy

Algorithm 3: Variant of Algorithm 1, SHED-LS-periodic

1 In Algorithm 1, substitute $\mathcal{I} = \{1\}$ with $\mathcal{I} = \{1, T, 2T, \dots\}$, for some input parameter $T < n$.

is restarted from the first EEPs of \mathbf{H}_{LS} , in what we call a periodic *renewal*. Differently from Algorithm 1, Algorithm 3 can not guarantee convergence in a finite number of steps, because $T < n$ and thus it could be that $c_t > 0$, $\forall t$ (see Theorem 3). We study the convergence rate of the algorithm by focusing on upper bounds on the Lyapunov exponent (Lyapunov, 1992) of the discrete-time dynamical system ruled by the descent algorithm. The Lyapunov exponent characterizes the rate of exponential (linear) convergence and it is defined as the positive constant $a_* > 0$ such that, considering $h(\boldsymbol{\theta}^t) := (\boldsymbol{\theta}^t - \boldsymbol{\theta}^*)a^{-t}$, if $a > a_*$ then $h(\boldsymbol{\theta}^t)$ vanishes with t , while if $a < a_*$, for some initial condition, $h(\boldsymbol{\theta}^t)$ diverges. The usual definition of Lyapunov exponent for discrete-time linear systems (see Czornik et al., 2012) is, considering the system defined in (5),

$$a_* := \limsup_{t \rightarrow \infty} \|\boldsymbol{\Psi}_t\|^{1/t}, \quad \boldsymbol{\Psi}_t = \mathbf{A}_1 \cdots \mathbf{A}_t. \quad (22)$$

From (14), we have that, for each k , $\|\mathbf{A}_k\| \leq c_k = (1 - \bar{\lambda}_n / \bar{\rho}_k)$. This implies that, defining

$$a_t := \left(\prod_{k=1}^t c_k \right)^{1/t}, \quad (23)$$

$$\bar{a} := \limsup_{t \rightarrow +\infty} a_t,$$

it is $a_* \leq \bar{a}$. The following Lemma formalizes this bound and provides an upper bound on the Lyapunov exponent obtained by applying Algorithm 3.

Lemma 7 *Let $c_k = (1 - \bar{\lambda}_n / \bar{\rho}_k)$ (see Eq. (15)). Applying Algorithm 3, the Lyapunov exponent of system (5) is such that*

$$a_* \leq \bar{a} = \limsup_{t \rightarrow +\infty} \left(\prod_{k=1}^t c_k \right)^{1/t}.$$

If $q_t^{(i)} = q_{t-1}^{(i)} + 1$, $\forall i, t$,

$$a_* \leq \bar{a}_T := \left(\prod_{k=1}^T c_k \right)^{1/T}. \quad (24)$$

where \bar{a}_T is such that $\bar{a}_{T+1} \leq \bar{a}_T$ and $\bar{a}_n = 0$.

Proof We see that $a_* \leq \bar{a}$ from definition (22), because for each k , $\|\mathbf{A}_k\| \leq c_k = (1 - \bar{\lambda}_n / \bar{\rho}_k)$. Now, we show that, if $q_t^{(i)} = q_{t-1}^{(i)} + 1$, $\forall i, t$, then $\bar{a} = \bar{a}_T$. To show this latter inequality, let us consider the logarithm of the considered values, so we prove $\log \bar{a} = \log \bar{a}_T$. Indeed, if $q_t^{(i)} = q_{t-1}^{(i)} + 1$ and applying Algorithm 3, c_k is a periodic sequence of the index k ($c_{k+T} = c_k$):

$$\begin{aligned}
 \log \bar{a} &= \limsup_t \frac{1}{t} \sum_{k=1}^t \log c_k \\
 &= \limsup_R \frac{1}{RT + T'} (R \sum_{k=1}^T \log c_k + \sum_{k=1}^{T'} \log c_k) \\
 &= \frac{1}{T} \sum_{k=1}^T \log c_k = \log \bar{a}_T
 \end{aligned} \tag{25}$$

where $R = \lfloor t/T \rfloor$ and $T' = t - RT$. ■

5. Federated learning with convex cost

Given the previous analysis and theoretical results for linear regression with quadratic cost, we are now ready to illustrate our Newton-type algorithm (Algorithm 4) for general convex FL problems, of which Algorithm 1 is a special case. We refer to this general version of the algorithm simply as SHED. Since in a general convex problem the Hessian depends on the current parameter, $\boldsymbol{\theta}^t$, we denote by $\mathbf{H}(\boldsymbol{\theta}^t)$ the global Hessian at the current iterate, while we denote by $\hat{\mathbf{H}}_t$ the global approximation, defined similarly to (12), with the difference that now eigenvalues and eigenvectors depend on the parameter for which the Hessian was computed.

The expression of $\hat{\mathbf{H}}_t$ thus becomes:

$$\hat{\mathbf{H}}_t = \frac{1}{M} \sum_{i=1}^M \hat{\mathbf{H}}_t^{(i)}(\boldsymbol{\theta}^{k_t^{(i)}}), \tag{26}$$

where $k_t^{(i)} \leq t$ denotes the iteration in which the local Hessian of agent i was computed. The parameter $\boldsymbol{\theta}^{k_t^{(i)}}$ is the parameter for which agent i computed the local Hessian, that in turn is being used for the update at iteration t .

The idea of the algorithm is to use previous versions of the Hessian rather than always recomputing it. This is motivated by the fact that as we approach the solution of the optimization problem, the second order approximation becomes more accurate and the Hessian changes more slowly. Hence, recomputing the Hessian and restarting the incremental approach provides less and less advantages as we proceed. From time to time, however, we need to re-compute the Hessian corresponding to the current parameter $\boldsymbol{\theta}^t$, because $\mathbf{H}(\boldsymbol{\theta}^{k_t})$ could have become too different from $\mathbf{H}(\boldsymbol{\theta}^t)$. As in Section 4.2, we call this operation a *renewal*. We denote by \mathcal{I} the set of iteration indices at which a renewal takes place. In principle, each agent could have its own set of renewal indices, and decide to recompute the Hessian matrix independently. In this work, we consider for simplicity that the set \mathcal{I} is the same for all agents, meaning that all agents use the same parameter for the local Hessian computation, i.e., $k_t^{(i)} = k_t, \forall i$. At the end of this section we describe heuristic strategies to choose \mathcal{I} with respect to the theoretical analysis. We remark that in the case of a quadratic cost, in which the Hessian is constant, one chooses $\mathcal{I} = \{1\}$, and so Algorithm 1 is a special

Algorithm 4: FL with convex cost - SHED

Input: $\{\mathcal{D}_i\}_{i=1}^M, t_{max}, \mathcal{I}, \boldsymbol{\theta}^0, \mathcal{A} = \{\text{agents}\}$
Output: $\boldsymbol{\theta}^{t_{max}}$

```

1 for  $t \leftarrow 0$  to  $t_{max}$  do
2   for agent  $i \in \mathcal{A}$  do
3     when Received  $\boldsymbol{\theta}^t$  from the Master do
4       if  $t \in \mathcal{I}$  then
5          $k_t \leftarrow t$ 
6         compute  $\mathbf{H}_t^{(i)} = \nabla^2 f^{(i)}(\boldsymbol{\theta}^t)$  // renewal
7          $\{(\hat{\lambda}_{j,t}^{(i)}, \hat{\mathbf{v}}_{j,t}^{(i)})\}_{j=1}^n \leftarrow \text{eigendec}(\mathbf{H}_t^{(i)})$  // eigendecomposition
8          $q_{t-1}^{(i)} \leftarrow 0$ 
9         compute  $\mathbf{g}_t^{(i)} = \mathbf{g}^{(i)}(\boldsymbol{\theta}^t) = \nabla f^{(i)}(\boldsymbol{\theta}^t)$ 
10        set  $d_t^{(i)}$  // according to CRs
11         $q_t^{(i)} \leftarrow q_{t-1}^{(i)} + d_t^{(i)}$  // increment
12         $\hat{\rho}_t^{(i)} \leftarrow \hat{\lambda}_{q_t^{(i)}+1,t}^{(i)}$  // approximation parameter
13         $U_t^{(i)} \leftarrow \{ \{ \hat{\mathbf{v}}_{j,t}^{(i)}, \hat{\lambda}_{j,t}^{(i)} \}_{j=q_{t-1}^{(i)}+1}^{q_t^{(i)}}, \mathbf{g}_t^{(i)}, \hat{\rho}_t^{(i)} \}$  // see (28) and (30)
14        Send  $U_t^{(i)}$  to the Master.
15
16 At the Master:
17 when Received  $U_t^{(i)}$  from all agents do
18   compute  $\hat{\mathbf{H}}_t^{(i)}, \forall i.$  // see (30)
19   Compute  $\hat{\mathbf{H}}_t$  (as in eq. (26)) and  $\mathbf{g}_t$ .
20   Get  $\eta_t$  via federated Armijo backtracking line search.
21   Perform Newton-type update (3).
22   Broadcast  $\boldsymbol{\theta}^{t+1}$  to all agents.
    
```

case of Algorithm 4.

The eigendecomposition can be applied to the local Hessian as before, we define

$$\hat{\mathbf{v}}_{j,t}^{(i)} = \mathbf{v}_j^{(i)}(\boldsymbol{\theta}^{k_t}), \quad \hat{\lambda}_{j,t}^{(i)} = \lambda_j^{(i)}(\boldsymbol{\theta}^{k_t}). \quad (27)$$

For notation convenience we also define

$$\tilde{\mathbf{v}}_{j,t}^{(i)} = (\hat{\lambda}_{j,t}^{(i)} - \hat{\rho}_t^{(i)})^{1/2} \hat{\mathbf{v}}_{j,t}^{(i)}, \quad (28)$$

The theoretical results on the convergence rate in this Section require that $\hat{\mathbf{H}}^{(i)}(\boldsymbol{\theta}) \geq \mathbf{H}^{(i)}(\boldsymbol{\theta}), \forall \boldsymbol{\theta}$, which in turn requires, defining $\hat{\rho}_t^{(i)} = \rho_t^{(i)}(\boldsymbol{\theta}^{k_t})$, that $\hat{\rho}_t^{(i)} \geq \hat{\lambda}_{q_t^{(i)}+1,t}^{(i)}$. Given the results of Theorem 1 on the range of the approximation parameter ρ_t achieving the best

convergence rate in the centralized least squares case, we set:

$$\hat{\rho}_t^{(i)} = \hat{\lambda}_{q_t+1,t}^{(i)}. \quad (29)$$

The local Hessian can be approximated as

$$\hat{\mathbf{H}}_t^{(i)}(\boldsymbol{\theta}^{k_t}) = \sum_{j=1}^{q_t^{(i)}} \tilde{\mathbf{v}}_{j,t}^{(i)} \tilde{\mathbf{v}}_{j,t}^{(i)T} + \hat{\rho}_t^{(i)} \mathbf{I}. \quad (30)$$

Clearly, it still holds that $\hat{\mathbf{H}}_t \geq \bar{\rho}_t \mathbf{I}$, $\forall t$, where $\bar{\rho}_t = \frac{1}{M} \sum_{i=1}^M \hat{\rho}_t^{(i)}$. Furthermore, it is easy to see that $\hat{\mathbf{H}}_t \leq K \mathbf{I}$, with K the smoothness constant of f . We assume to use Armijo backtracking condition, that is recalled in Algorithm 2.

Theorem 8 *For any initial condition, Algorithm 2 ensures convergence to the optimum, i.e.,*

$$\lim_{t \rightarrow +\infty} \|\boldsymbol{\theta}_t - \boldsymbol{\theta}^*\| = 0.$$

Proof See Appendix A. ■

Now, we provide results related to the convergence rate of the algorithm. In order to prove the following results, we need to impose some constraints on the renewal indices set \mathcal{I} . Specifically,

Assumption 3 *Denoting $\mathcal{I} = \{C_j\}_{j \in \mathbb{N}}$, there exists a finite positive integer \bar{l} such that $C_j \leq C_{j-1} + \bar{l}$, $\forall j$. This is equivalent to state that, writing $k_t = t - \tau$, the ‘delay’ τ is bounded.*

The next Theorem provides a bound describing the relation between the convergence rate and the increments of outdated Hessians.

Theorem 9 *Applying SHED (Algorithm 4), for any iteration t , it holds that:*

$$\|\boldsymbol{\theta}^{t+1} - \boldsymbol{\theta}^*\| \leq c_{1,t} \|\boldsymbol{\theta}^t - \boldsymbol{\theta}^*\| + c_{2,t} \|\boldsymbol{\theta}^t - \boldsymbol{\theta}^*\|^2 \quad (31)$$

where, defining $\bar{\lambda}_{n,t} = \frac{1}{M} \sum_{i=1}^M \hat{\lambda}_{n,t}^{(i)}$ and $\bar{\rho}_t = \frac{1}{M} \sum_{i=1}^M \hat{\rho}_t^{(i)}$ (see (27) and (29)),

$$\begin{aligned} c_{1,t} &= \left(1 - \frac{\bar{\lambda}_{n,t}}{\bar{\rho}_t}\right) + \frac{L}{\bar{\rho}_t} \|\boldsymbol{\theta}^t - \boldsymbol{\theta}^{k_t}\| + (1 - \eta_t) \frac{\|\mathbf{H}(\boldsymbol{\theta}^t)\|}{\bar{\rho}_t}, \\ c_{2,t} &= \frac{\eta_t L}{2\bar{\rho}_t}. \end{aligned} \quad (32)$$

Proof The beginning of the proof follows from the proof of Lemma 3.1 in Erdogdu and Montanari (2015), (see page 18). In particular, we can get the same inequality as (A.1) in Erdogdu and Montanari (2015) (the \mathbf{Q}^t here is $\hat{\mathbf{H}}_t$) with the difference that since we are

not sub-sampling, we have (using the notation of Erdogdu and Montanari (2015)) $S = [n]$. The following inequality holds:

$$\begin{aligned} \|\boldsymbol{\theta}^{t+1} - \boldsymbol{\theta}^*\| &\leq \|\boldsymbol{\theta}^t - \boldsymbol{\theta}^*\| \|I - \eta_t \hat{\mathbf{H}}_t^{-1} \mathbf{H}(\boldsymbol{\theta}^t)\| \\ &\quad + \eta_t L \frac{\|\hat{\mathbf{H}}_t^{-1}\|}{2} \|\boldsymbol{\theta}^t - \boldsymbol{\theta}^*\|^2. \end{aligned}$$

Note that, as we have shown in the proof of Theorem 3, it holds $\|\hat{\mathbf{H}}_t^{-1}\| \leq 1/\bar{\rho}_t$. We now focus on the first part of the right hand side of the inequality:

$$\begin{aligned} \|I - \eta_t \hat{\mathbf{H}}_t^{-1} \mathbf{H}(\boldsymbol{\theta}^t)\| &\leq \|\hat{\mathbf{H}}_t^{-1}\| (\|\hat{\mathbf{H}}_t - \mathbf{H}(\boldsymbol{\theta}^t)\| \\ &\quad + (1 - \eta_t) \|\mathbf{H}(\boldsymbol{\theta}^t)\|) \\ &\leq \frac{1}{\bar{\rho}_t} \|\hat{\mathbf{H}}_t - \mathbf{H}(\boldsymbol{\theta}^t)\| + \frac{(1 - \eta_t)}{\bar{\rho}_t} \|\mathbf{H}(\boldsymbol{\theta}^t)\| \end{aligned}$$

and focusing now on the first term of the right hand side of the last inequality

$$\begin{aligned} &\frac{1}{\bar{\rho}_t} (\|\hat{\mathbf{H}}_t - \mathbf{H}(\boldsymbol{\theta}^{k_t})\| + \|\mathbf{H}(\boldsymbol{\theta}^t) - \mathbf{H}(\boldsymbol{\theta}^{k_t})\|) \\ &\leq \frac{1}{\bar{\rho}_t} \left(\frac{1}{M} \sum_{i=1}^M \|\hat{\mathbf{H}}_t^{(i)}(\boldsymbol{\theta}^{k_t}) - \mathbf{H}^{(i)}(\boldsymbol{\theta}^{k_t})\| + L \|\boldsymbol{\theta}^{k_t} - \boldsymbol{\theta}^t\| \right) \\ &= 1 - \frac{\bar{\lambda}_{n,t}}{\bar{\rho}_t} + \frac{L}{\bar{\rho}_t} \|\boldsymbol{\theta}^{k_t} - \boldsymbol{\theta}^t\|, \end{aligned}$$

where the last equality holds being $\|\hat{\mathbf{H}}_t^{(i)}(\boldsymbol{\theta}^{k_t}) - \mathbf{H}^{(i)}(\boldsymbol{\theta}^{k_t})\| = \hat{\rho}_t^{(i)} - \lambda_{n,t}^{(i)}$, which in turn is true given that $\hat{\rho}_t^{(i)} = \hat{\lambda}_{q_t^{(i)}+1,t}^{(i)}$. \blacksquare

The above theorem is a generalization of Lemma 3.1 in Erdogdu and Montanari (2015) (without sub-sampling). In particular, the difference is that (i) the dataset is distributed and (ii) an outdated Hessian matrix is used.

Theorem 10 *Recall the definition of the average strong convexity constant $\bar{\kappa} = (1/M) \sum_{i=1}^M \kappa_i$, with κ_i the strong convexity constant of agent i . Let K be the smoothness constant of f . The following results hold:*

1. If

$$3\bar{\kappa}(M(t) + \|\boldsymbol{\theta}^t - \boldsymbol{\theta}^*\|) + K\|\boldsymbol{\theta}^t - \boldsymbol{\theta}^*\| \leq \frac{3\bar{\kappa}^2}{L}(1 - 2\alpha), \quad (33)$$

and

$$\frac{3}{2}L\|\boldsymbol{\theta}^t - \boldsymbol{\theta}^*\| + LM(t) \leq \bar{\kappa} \quad (34)$$

with $M(t) = \max\{\|\boldsymbol{\theta}^t - \boldsymbol{\theta}^*\|, \|\boldsymbol{\theta}^{k_t} - \boldsymbol{\theta}^*\|\}$ then SHED (Algorithm 4) enjoys at least linear convergence.

2. Define $\mathcal{X}_t := \{k \leq t : \bar{\rho}_k = \bar{\lambda}_{n,k}\}$. Let $|\mathcal{X}_t|$ denote the cardinality of \mathcal{X}_t . If $|\mathcal{X}_t| = 0$ then SHED enjoys linear convergence and the Lyapunov exponent of the estimation error can be upper bounded as

$$a_* \leq \limsup_t \left(\prod_{k=1}^t 1 - \frac{\bar{\lambda}_n^o}{\bar{\rho}_k^o} \right)^{1/t} \quad (35)$$

where $\bar{\lambda}_n^o$ and $\bar{\rho}_k^o$ are the average of the n -th eigenvalues and approximation parameters, respectively, computed at the optimum:

$$\bar{\lambda}_n^o = \frac{1}{M} \sum_{i=1}^M \lambda_n^{(i)}(\boldsymbol{\theta}^*), \quad \bar{\rho}_k^o = \frac{1}{M} \sum_{i=1}^M \rho_k^{(i)o},$$

with $\rho_k^{(i)o} = \lambda_{q_k^{(i)}+1}^{(i)}(\boldsymbol{\theta}^*)$.

3. Let $|\mathcal{X}_t|$ denote the cardinality of \mathcal{X}_t . If $|\mathcal{X}_t| \geq t^{1/2}h(t)$, with $h(t)$ any function such that $h(t) \rightarrow \infty$ as $t \rightarrow \infty$, then the Lyapunov exponent is $a_* = 0$ and thus SHED enjoys super-linear convergence.

Proof [Sketch of proof] For 1), we first show that when condition (33) holds, the step size is chosen equal to one by the Armijo backtracking line search. We then show that when also (34) holds, then the cost converges at least linearly for any subsequent iteration. For 2), we upper bound the Lyapunov exponent and exploit local Lipschitz continuity to provide the result. For 3), we exploit at least linear convergence proved in 1) together with the assumption on the cardinality of the set \mathcal{X}_t . For the complete proof see Appendix A. ■

In the above theorem we have shown that SHED enjoys at least linear convergence and provided a sufficient condition on the choice of renewals indices set to guarantee super-linear convergence. The sufficient condition could be easily guaranteed for example with a choice of periodic renewals with a period such that the cardinality of \mathcal{X}_t is big enough. Note that in the case in which all agents send one EEP at each iteration we can get an explicit expression for the Lyapunov exponent also in the convex cost case, getting

$$a_* \leq \bar{a}_T := \prod_{k=1}^T \left(1 - \frac{\bar{\lambda}_n^o}{\bar{\rho}_k^o} \right)^{1/T}. \quad (36)$$

5.1 Heuristics for the choice of \mathcal{I}

From the theoretical results provided above we can do a heuristic design for the renewal indices set \mathcal{I} . In particular, we see from the bound (31) in Theorem 9 that when we are at the first iterations of the optimization we would frequently do the renewal operation, given that the Hessian matrix changes much faster and that the term $\|\boldsymbol{\theta}^{kt} - \boldsymbol{\theta}^t\|$ is big. As we converge, instead, we would like to reduce the number of renewal operations, to improve the convergence rate, and this is strongly suggested by the result 2) related to the Lyapunov exponent in Theorem 10. Furthermore, the super-linear convergence that follows from 3)

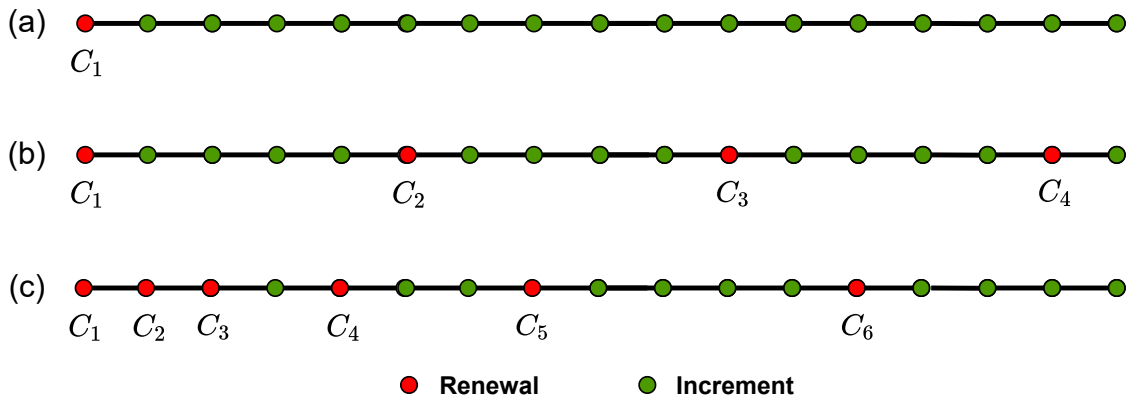


Figure 3: Illustration of possible choices of renewal indices set. The set $\mathcal{I} = \{C_j\}$ specifies the iterations at which a renewal takes place. (a) illustrates the least squares case in which renewal is performed only once, see Algorithm 1, (b) the periodic renewals case with $T = 5$, so $\mathcal{I} = \{1, 5, 10, \dots\}$, see Algorithm 3, and (c) the set in which the distance between renewals increases according to the Fibonacci sequence.

in the same Theorem suggests to keep performing renewals in order to let the cardinality of \mathcal{X}_t to grow sufficiently fast with t .

To evaluate SHED performance, we obtain the results of the next section using two different renewal strategies. In the first we choose the distance between renewals to be determined by the *Fibonacci* sequence, so $\mathcal{I} = \{C_j\}$, where $C_j = \sum_{k=1}^j F_k$, F_k being the *Fibonacci* sequence, with $F_0 = 0, F_1 = 1$. When the sequence C_j reaches $n - 1$, the next values of the sequence are chosen so that $C_{j+1} = C_j + n - 1$. We will call this method Fib-SHED. The second strategy is based on the inspection of the value of the gradient norm, $\|\mathbf{g}_t\|$, which is directly related to $\|\boldsymbol{\theta}^t - \boldsymbol{\theta}^*\|$. In particular, we will make a decision concerning renewals at each iteration by evaluating the empirically observed decrease in the gradient norm. If $\|\mathbf{g}_t\| - \|\mathbf{g}_{t-1}\| < b(\|\mathbf{g}_{t-1}\| - \|\mathbf{g}_{t-2}\|)$ for some constant b , this strategy triggers a renewal. To guarantee at least linear convergence, we impose a renewal after n iterations in which no renewal has been triggered. In the rest of the paper we call this strategy GN-SHED (Gradient Norm-based SHED). See Fig. 3 for an illustration of some different possible choices for the renewal indices sets.

6. Empirical Results

In this section we present empirical results obtained with real datasets. In particular, to illustrate Algorithm 1, thus in the case of regression via least squares, we consider the popular Million Song (1M Songs) Dataset Bertin-Mahieux et al. (2011) and the Online News Popularity dataset Fernandes et al. (2015), both taken from the UCI Machine Learning Repository Dua and Graff (2017). For the more general non linear convex case, we apply logistic regression to two image datasets, in particular the FMNIST Xiao et al. (2017) and

EMNIST digits Cohen et al. (2017) datasets, and to the ‘w8a’ web page dataset available from the libSVM library Chang and Lin (2011). First, we show performance assessments related to the theoretical results of the previous sections. In particular, we show how the versatility of the algorithm applies effectively to the FL framework, showing results related to parameters choice and heterogeneity of CRs. Finally, we compare our algorithm against state-of-the-art approaches in both i.i.d. and non i.i.d. data distributions, showing the advantage that can be provided by our approach, especially in the case of heterogeneous CRs. When comparing with other algorithms, we provide results for both i.i.d. and non i.i.d. partitions to show that our algorithm is competitive with state-of-the-art approaches also in the i.i.d. configuration.

In the general convex case, we follow the heuristics discussed at the end of Section 5, where the version using the Fibonacci sequence to define \mathcal{I} is called Fib-SHED while the event-triggered one based on the gradient norm inspection is called GN-SHED. As done previously in the paper, Algorithm 1 is referred to as SHED-LS, and Algorithm 4 as SHED, while their periodic variants (Algorithm 3), are referred to as SHED-LS-periodic and SHED-periodic, respectively. If the value of $d_t^{(i)}$ is not specified, SHED-LS and SHED stand for the proposed approach when $d_t^{(i)} = 1$ for each iteration t and agent i , $i = 1, \dots, M$.

In this section, we show results for $\mu = 10^{-5}, 10^{-6}, 10^{-8}$, and we have obtained similar results with $\mu = 10^{-4}$. Note that $10^{-4}, 10^{-6}, 10^{-8}$ were the values considered in Wang et al. (2018).

6.1 Datasets

We consider the following datasets. For each dataset, we partition the dataset for the FL framework in both an i.i.d. and non i.i.d. way. In particular:

6.1.1 LEAST SQUARES

We consider the popular Million Song Dataset Bertin-Mahieux et al. (2011). The objective of the regression is the prediction of the year in which a song has been recorded. The dataset consists in 515K dated tracks starting from 1922 recorded songs. We take a subset of 300K tracks as training set. The feature size of each data sample is $n = 90$. As preprocessing of the dataset we apply rescaling of the features and labels to have them comprised between 0 and 1. To get a number of samples per agent in line with typical federated learning settings, we spread the dataset to $M = 200$ agents, so that each agent has around 800 data samples.

As a non i.i.d configuration, we consider a scenario with *label distribution skew* and unbalancedness (see Kairouz et al. (2021)). In particular, we partition the dataset so that each agent has songs from only one year, and different number of data samples. In this configuration, some agent has a very small number of data samples, while other agents have up to 11K data samples.

We also provide some results using the Online News Popularity Fernandes et al. (2015), made of 40K online news data samples. The target of the prediction is the number of shares given processed information about the online news. Data is processed analogously to 1M Songs. $M = 30$ agents are considered with 500 data sample each.

6.1.2 LOGISTIC REGRESSION

To validate our algorithm with a non linear convex cost we use two popular and widely adopted image datasets and a web page prediction dataset.

Image datasets: We consider the FMNIST (Fashion-MNIST) dataset Xiao et al. (2017), and the EMNIST (Extended-MNIST) digits dataset Cohen et al. (2017). For both, we consider a training set of 60K data samples. We apply standard pre-processing to the datasets: we rescale the data to be between 0 and 1 and apply PCA Sheikh et al. (2020), getting a parameter dimension of $n = 300$. Given that the number of considered data samples is smaller with respect to 1M-Songs, we distribute the dataset to $M = 28$ agents.

We focus on one-vs-all binary classification via logistic regression, which is the basic building block of multinomial logistic regression for multiclass classification. In a one-vs-all setup, one class (that we call target class), needs to be distinguished from all the others. The i.i.d. configuration is obtained by uniformly assigning to each agent samples from the target class and mixed samples of the other classes. When the agents perform one-vs all, we provide them with a balanced set where half of the samples belong the target class, and the other half to the remaining classes, equally mixed. In this way, each agent has around 400 data samples.

To partition the FMNIST and EMNIST datasets in a non i.i.d. way, we provide each agent with samples from only two classes: one is the target class and the other is one of the other classes. This same approach was considered in Li et al. (2020b). In this section we show results obtained with a target class corresponding to label 'one' of the dataset, but we have seen that equivalent results are obtained choosing one of the other classes as target class.

Web page dataset: We consider the web page category prediction dataset 'w8a', available from libSVM Chang and Lin (2011). The dataset comprises 50K data samples and the objective of the prediction is the distinction between two classes, depending on the website category. The dataset is already pre-processed. Being a binary and strongly unbalanced dataset, we do not consider an i.i.d. configuration, and spread the dataset to the agents similarly to the case of FMNIST, with the difference that some agent only has data samples from one class. The number of data samples per agent is between 700 and 900.

6.2 Federated backtracking

To tune the step size when there are no guarantees that a step size equal to one decreases the cost, we adopt the same strategy adopted in Wang et al. (2018): an additional communication round takes place in which each agent shares with the master the loss obtained when the parameter is updated via the new descent direction for different values of the step size. In this way, we can apply a distributed version of the popular Armijo backtracking line search (see Algorithm 2 or Boyd and Vandenberghe (2004), page 464). When showing the results with respect to communication rounds, we always include also the additional communication round due to backtracking.

6.3 Heterogeneous channels model

As previously outlined, our algorithm is suitable for FL frameworks in which agents have heterogeneous transmission resources, that is for instance the case in Federated Edge Learning. As an example we consider the case of wireless channels, that are characterized by strong variability. In particular, in the wireless channel subject to fading conditions and interference, at each communication round agents could have very different CRs available Pase et al. (2021); Wadu et al. (2020); Chen et al. (2020). To show the effectiveness of our algorithm in such a scenario, we consider the Rayleigh fading model. In a scenario with perfect channel knowledge, in which agent i allocates a certain bandwidth $B^{(i)} = B$ (we consider it to be the same for all agents) to the FL learning task, we have that the achievable rate of transmission for the i -th user is:

$$R^{(i)} = B \log_2(1 + \gamma\Gamma^{(i)}) \quad (37)$$

where $\Gamma^{(i)}$ is a value related to transmission power and environmental attenuation for user i . For simplicity we fix $\Gamma^{(i)} = \Gamma = 5$ for all users (in Pase et al. (2021), for instance, $\Gamma = 1$ and $\Gamma = 10$ were considered). The only source of variability is then $\gamma \sim \text{Exp}(\nu)$, modeling the Rayleigh fading effect. We fix $\nu = 1$.

With respect to our algorithm, for illustration purposes, we compare scenarios in which the number of vectors in \mathbb{R}^n related to second order information, $d_t^{(i)}$, is deterministically chosen and fixed for all users, with a scenario in which $d_t^{(i)}$ is randomly chosen for each round for each user. In particular, we fix:

$$d_t^{(i)} = d_\gamma := \lfloor d_0 \log_2(1 + \gamma\Gamma) \rfloor. \quad (38)$$

This would correspond to each user allocating a bandwidth of $B = d_0 B_0$ to the transmission of second order information, where B_0 is the transmission speed needed to transmit a vector in \mathbb{R}^n per channel use. In the rest of the paper, we fix $d_0 = 2$. This implies that in average the number of vectors that an agent is able to transmit is 4, and the actual number can vary from 0 (only the gradient is sent) to 10. For simplicity, when adopting this framework, we assume that agents are always able to send at least a vector in \mathbb{R}^n per communication round (so the gradient is always sent). Further simulations are left as future work.

6.4 Choice of ρ_t

In Fig. 4 we analyze the optimization performance with respect to the choice of the approximation parameter ρ_t , following the theoretical results of Section 3.1, in particular Theorem 1 and Corollary 2. We provide performance analysis in the distributed setting for least squares with the 1M Song and Online News Popularity datasets in (a) and (b), respectively. We show the error $\|\theta^t - \theta^*\|$ versus the number of communication rounds. We adopt the notation of Section 5 as it includes least squares as a special case. In this subsection, the same parameter choice is done for all the agents, thus we omit to specify that the parameter is specific of the i -th agent. We compare two choices for the approximation parameter: (i) the one providing the best estimation error according to Corollary 2, $\rho_t^* = (\hat{\lambda}_{q_t+1,t} + \hat{\lambda}_{n,t})/2$ with the step size $\eta_t = 1$, and (ii) the one that was proposed in Erdogdu and Montanari (2015), where $\rho_t = \hat{\lambda}_{q_t+1,t}$. In the latter case, following the result of Theorem 1 related to

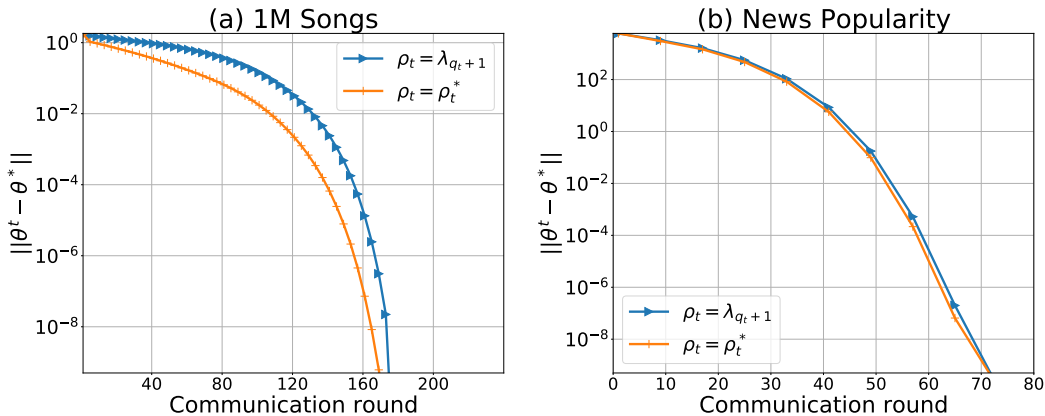


Figure 4: Performance comparison for different values of ρ_t . The best choice in terms of estimation error from Corollary 2 is compared against the choice that was proposed in Erdogdu and Montanari (2015), that is $\rho_t = \lambda_{q_t+1}$

the best convergence rate we pick the step size to be equal to the η_t^* in Eq. (11). From the plots, we can see the improvement provided by the choice of ρ_t^* against $\hat{\lambda}_{q_t+1,t}$, although the performance is very similar for both values of the approximation parameter.

6.5 Lyapunov exponent convergence bound

In Fig. 5, we illustrate how the Lyapunov exponent bounds derived in Sec. 4.2 and Theorem 10-2) characterize the linear convergence rate of the algorithms. In particular, we consider the cases of periodic renewals in both the least squares and logistic regression case, considering the case in which $q_t^{(i)} = q_{t-1}^{(i)} + 1, \forall i, t$ and renewals are periodic with period T . The plots show how the linear convergence rate is dominated by the Lyapunov exponent bound characterized by \bar{a}_T . For illustrative purposes, we show the results for the choice of $T = 35$ and of $T = 25$ for least squares on 1M songs and logistic regression on FMNIST, respectively.

6.6 Role of d_t

In Figure 6, we show the impact of each agent transmitting more eigenvalue-eigenvector pairs per communication rounds, showing the optimization results when the increment, $d_t^{(i)}$, takes different values. In this subsection, for illustration purposes, renewals of SHED are determined by the Fibonacci sequence (see Sec. 5.1). We consider the case when the number is the same and fixed (specifically we consider $d_t^{(i)} \in \{1, 3, 6, 30\}$) for all the agents and the case $d_t^{(i)} = d_\gamma$, where d_γ is as defined in Eq. (38), with $d_0 = 2$ and $\Gamma = 5$, that means that in average d_γ is equal to 4. In this latter case each agent is able to transmit a different random number of eigenvalue-eigenvector pairs. This configuration is relevant as our algorithm allows agents to contribute to the optimization according to their specific communication resources (CRs). In Figures 6-(a)-(c) we show the results for the least squares on 1M Songs, while in Figures 6-(b)-(d) we show the results in the convex case

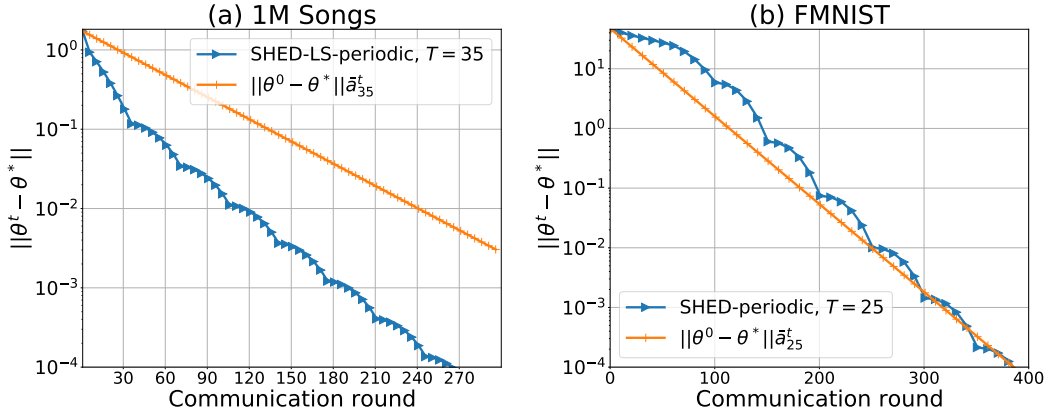


Figure 5: Linear convergence with periodic renewals illustrated via the study of the upper bound on the dominant Lyapunov exponent of the estimation error from equation (23) and point 2) of Theorem 10. \bar{a}_T is as in eqs. (23) and (36) for (a) and (b), respectively. Note that the upper bound is on the slope of the decreasing cost.

of logistic regression on the FMNIST dataset. We can see from Figures 6-(a)-(b) how the global number of communication rounds needed for convergence can be significantly reduced by increasing the amount of information transmitted at each round. In particular, at each round, the number of vectors in \mathbb{R}^n being transmitted is $d_t + 1$, since together with the d_t scaled eigenvectors, $\{\tilde{\mathbf{v}}_{j,t}^{(i)}\}_{j=q_{t-1}^{(i)}+1}^{q_t^{(i)}}$ (see Algorithm 2), agents need to transmit also the gradient. In the least squares case, the number of iterations needed for convergence is surely smaller than the number of EEPs sent: when the $n - 1$ -th EEP has been shared, convergence surely occurs. When the number of EEPs is random (d_γ), but equal to 4 in average, we see that we can still get a significant improvement, which is between the choices $d_t = 3$ and $d_t = 6$.

Let us now analyze the case of logistic regression. In Figures 6-(b)-(d) we emphasize the role of the *renewal* operation, showing also how incrementally adding eigenvectors of the outdated Hessian improves the convergence, as formalized and shown in Theorems 9 and 10. In particular, from Figure 6-(b) it is possible to appreciate the impact of increasing the interval between renewals.

Quantifying the improvement provided by the usage of greater increments analyzing the empirical results, we see that when $d_t = 3$, the number of vectors transmitted per round is 4, against the 2 transmitted when $d_t = 1$, so the communication load per round is twice as much. We see that, despite this increase in data transmitted per round, in the case $d_t = 3$ the overall number of communication rounds is halved with respect to the case $d_t = 1$. An equivalent result occurs for the case $d_t = 6$. Notably, for the case $d_t = d_\gamma$, with an average increment equal to 4, we see that the convergence speed is in between the cases $d_t = 3$ and $d_t = 6$, which shows the effectiveness of the algorithm under heterogeneous channels. For $d_t = 30$, even if we increase the communication by a factor 15, we get a convergence that is only 10 times faster. This is of interest because it shows that if we increase arbitrarily the increment d_t , we pay in terms of overall communication load.

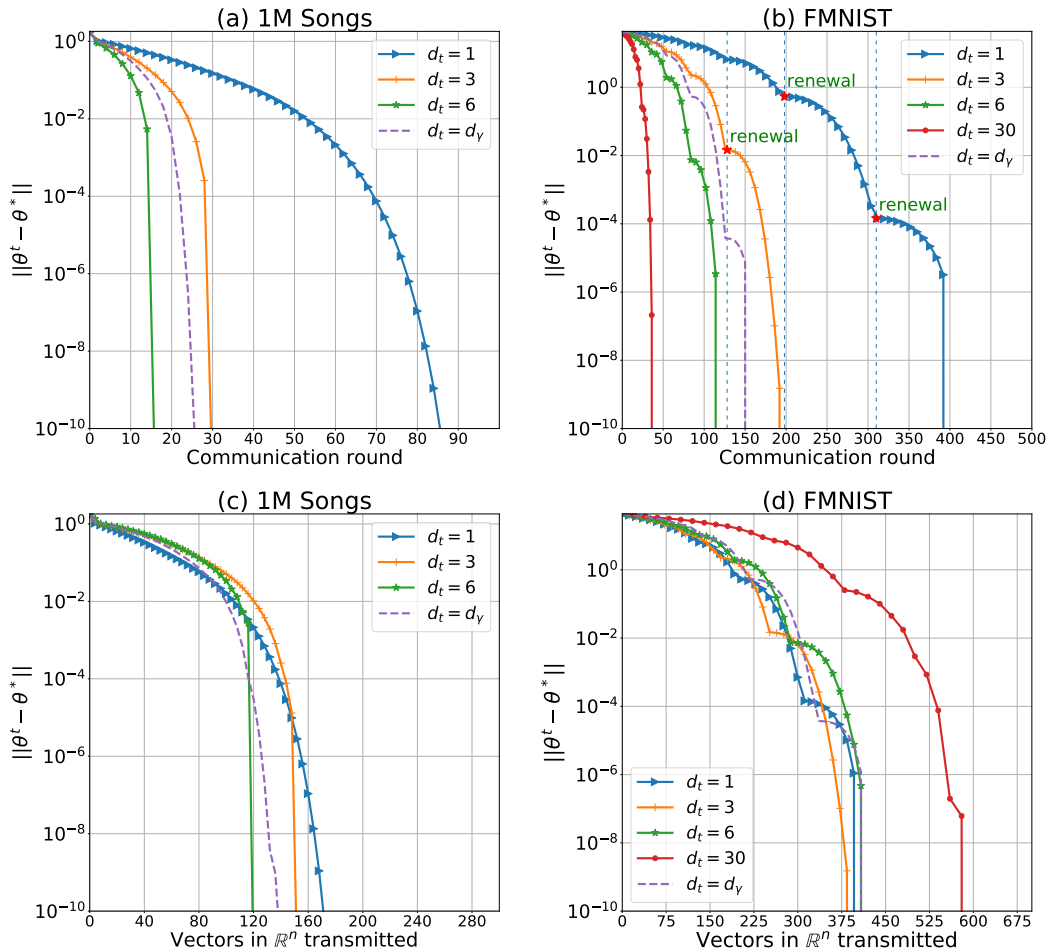


Figure 6: Performance comparison for different values of d_t for (i) linear regression on 1M Songs ((a) and (c)) and (ii) logistic regression on FMNIST ((b) and (d)). d_γ is as defined in Eq. (38), with $d_0 = 2$, so d_γ is in average equal to 4. In (b), we emphasize three points where the renewal operation (see Algorithm 4) takes place.

In Figures 6-(c)-(d) we plot the error as a function of the amount of data transmitted per agent, where the number of vectors in \mathbb{R}^n is the unit of measure. These plots show that, for small values of d_t (in particular, $d_t \in \{1, 3, 6\}$), the overall data transmitted does not increase for the considered values of d_t , meaning that we can significantly reduce the number of global communication rounds by transmitting more data per round without increasing the overall communication load. This is true in particular also for the case $d_t = d_\gamma$, thus when the agents' channels availability is heterogeneous at each round, showing that our algorithm works even in this relevant scenario without increasing the communication load. On the other hand, in the case of $d_t = 30$, if we increase the amount of information by

an order of magnitude, even if we get to faster convergence, we have as a consequence a significant increase in the communication load that the network has to take care of.

6.7 Comparison against other algorithms

In this subsection, SHED-LS+ and SHED+ signifies that the number of Hessian EEPs is chosen randomly for each agent i , according to the model for simulating heterogeneous CRs illustrated in Sec. 6.3, so $d_t^{(i)} = d_\gamma$, with an average increment equal to 4. To distinguish the different heuristic strategies for the renewals indices set, we use Fib-SHED to denote the approaches where \mathcal{I} is pre-determined by the Fibonacci sequence, while GN-SHED to denote the approach in which renewals are event-triggered by the gradient norm inspection (see Sec. 5.1)

We compare the performance of our algorithm with a state-of-the art first-order method, accelerated gradient descent (AGD, with the same implementation of Wang et al. (2018)).

As benchmark second-order methods we consider the following:

- a distributed version of the Newton-type method proposed in Erdogdu and Montanari (2015), to which we refer as Mont-Dec, which is the same as Algorithm 4 with the difference that the renewal occurs at each communication round, so the Hessian is always recomputed and the second-order information is never outdated. In this way, the eigenvectors are always the first $(\{v_{j,t}\}_{j=1}^{d_t})$, so this algorithm is neither incremental nor exploits outdated second-order information. We fix the amount of second-order information sent by the agents to be the same as the previously described SHED+.
- the distributed optimization state-of-the-art NT approach exploiting the harmonic mean, GIANT Wang et al. (2018). While in GIANT the local Newton direction is computed via conjugate gradient method, in DONE T. Dinh et al. (2022), a similar approach has been proposed but using Richardson iterations. To get our results, we provide the compared algorithm with the actual exact harmonic mean, so that we include both the algorithms at their best. Referring to this approach, we write GIANT in the figures. We remark that GIANT requires an extra communication round, because the algorithm requires the agents to get the global gradient. We also implemented the determinantal averaging approach Dereziński and Mahoney (2019) to compensate for the inversion bias of the harmonic mean, but we did not see notable improvements so we do not show its results for the sake of plot readability.
- the very recently proposed FedNL method presented in Safaryan et al. (2021). We adopted the best performing variant (FedNL-LS), with rank-1 matrix compression, which initializes the Hessian at the master with the complete Hessian computed at the initial parameter value, so the transmission of the Hessian matrix $\mathbf{H}(\boldsymbol{\theta}^0)$ at the first round is required. This method requires the computation of the Hessian and of an $n \times n$ matrix SVD at each iteration. FedNL uses the exact same amount of CRs as SHED (so with $d_t^{(i)} = 1, \forall i$), as it sends the gradient and one eigenvector at each iteration. For the Hessian learning step size, we adopt the same choice of Safaryan et al. (2021) (step size equal to 1), and we observed that different values of this parameter did not provide improvements.

We do not compare Mont-Dec and FedNL in the least squares case, as these algorithms are specifically designed for a time-varying Hessian and it does not make sense to use them in a least squares problem.

In the following, we show the details of results for the least squares on 1M Songs dataset and then for logistic regression on the FMNIST dataset. The detailed Figures of convergence results obtained with the EMNIST digits and ‘w8a’ are provided in Appendix B, while a summary of the results obtained on all the considered datasets is provided in Section 6.7.3.

6.7.1 LEAST SQUARES ON 1M SONGS

In Fig. 7 we show the performance of the algorithm in the case of least squares applied on the 1M Songs dataset (thus the procedure is the one described in Algorithm 1). We plot the relative cost $f(\theta^t) - f(\theta^*)$ versus the communication rounds. We see that AGD is characterized by very slow convergence due to the high condition number. Together with AGD, in Fig. 7 we show three Newton-type approaches: the state-of-the-art GIANT Wang et al. (2018), SHED and SHED+. We see how in the i.i.d. case GIANT performs well even if SHED+ is the fastest, but all the three algorithms have similar performance compared to the first-order approach (AGD). In the non i.i.d. case, whose framework has been described in Sec. 6.1.1, we can see how GIANT has a major performance degradation, even if still obtaining a better performance with respect to first-order methods. On the other hand, both SHED and SHED+ do not show performance degradation in the non i.i.d. case.

6.7.2 LOGISTIC REGRESSION ON FMNIST

In Figs. 8, 9 we show the results obtained with the FMNIST dataset with the setup described in Sec. 6.1.2. We show the performance for two values of the regularization parameter, μ , in particular $\mu = 10^{-5}$ and $\mu = 10^{-6}$. We compare our approach (Algorithm 4, SHED) also

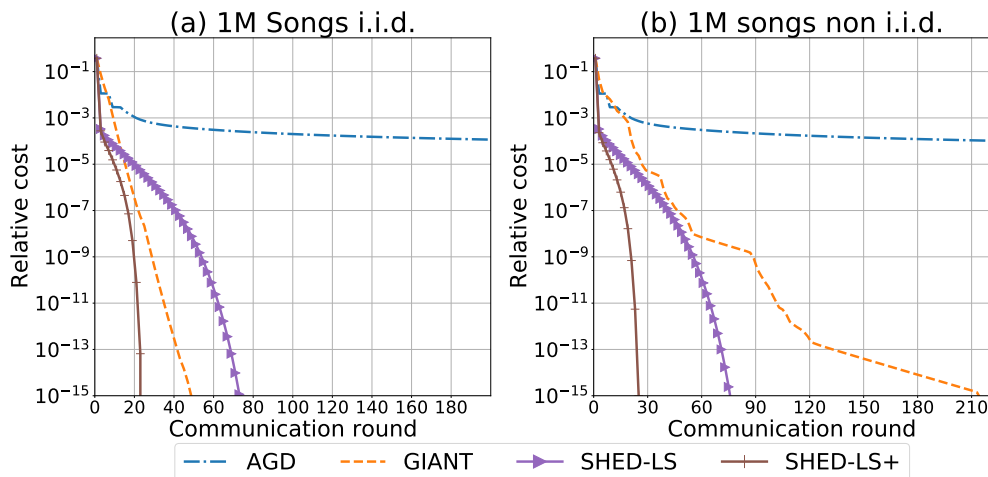


Figure 7: Performance comparison for least squares on 1M Songs. Relative cost is $f(\theta^t) - f(\theta^*)$. For SHED-LS and SHED-LS+, see Algorithm 1

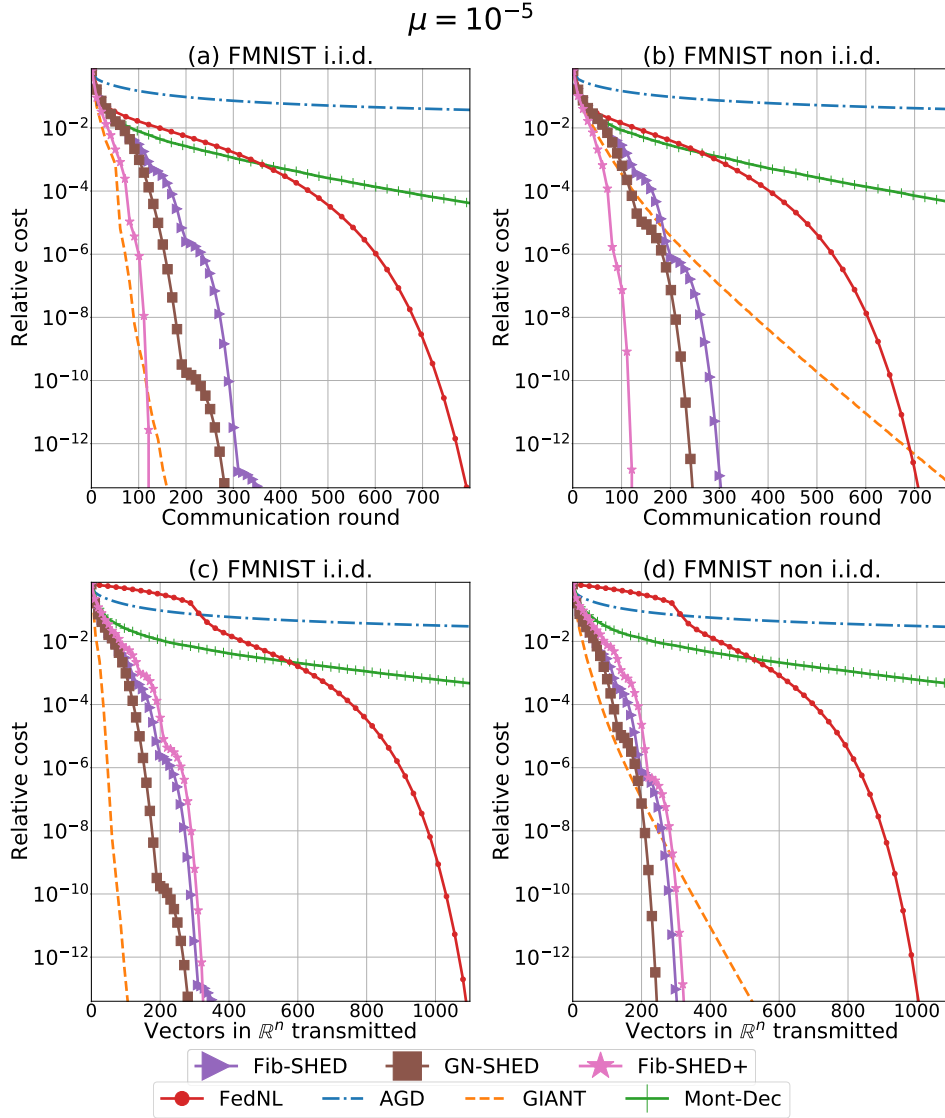


Figure 8: Performance comparison of logistic regression on FMNIST when $\mu = 10^{-5}$. Relative cost is $f(\boldsymbol{\theta}^t) - f(\boldsymbol{\theta}^*)$.

against FedNL and Mont-Dec. We show the performance of Fib-SHED, Fib-SHED+ and GN-SHED. As we did for Fig. 6, to provide a complete comparison, in Figs. 8-9-(c)-(d) we show also the relative cost versus the overall amount of data transmitted, in terms of overall number of vectors in \mathbb{R}^n transmitted. From Fig. 8-(a)-(b), we can see how also in the FMNIST case the non i.i.d. configuration causes a performance degradation for GIANT, while SHED and FedNL are not impacted.

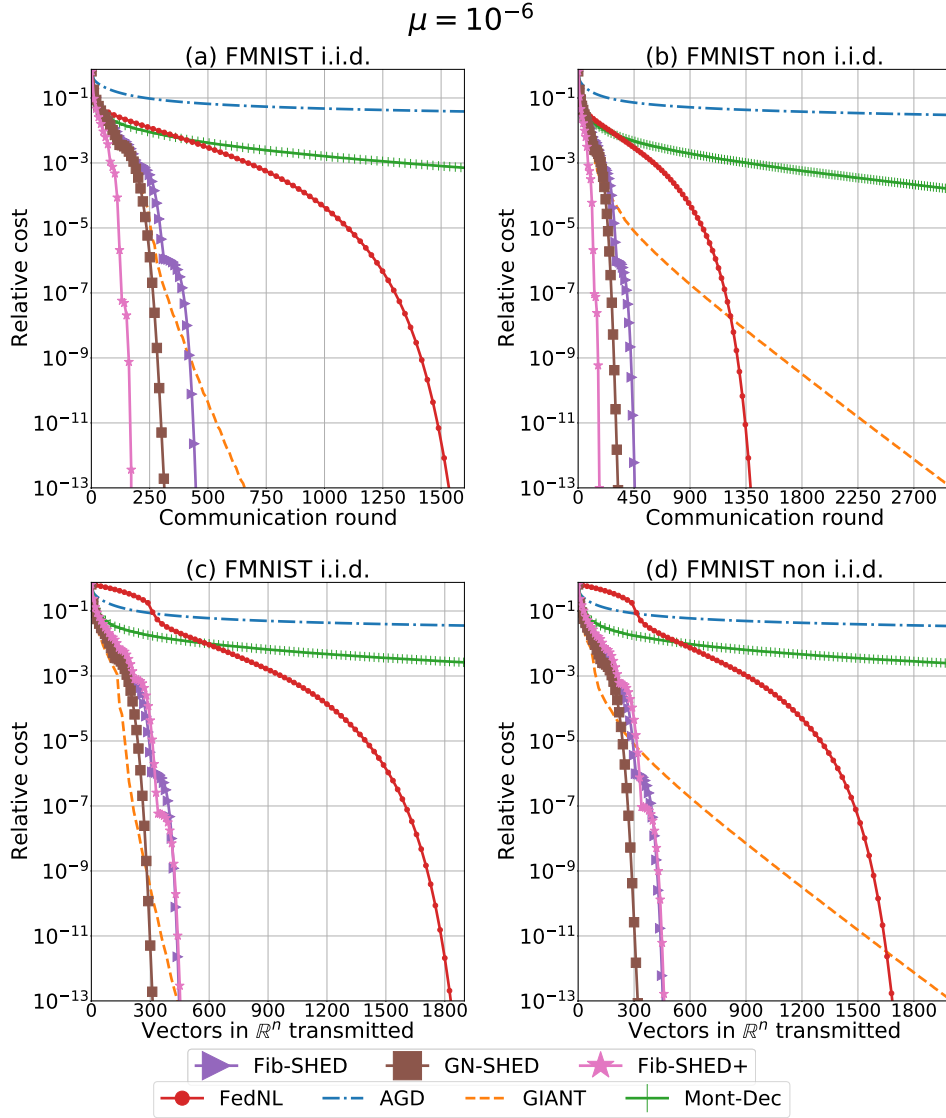


Figure 9: Performance comparison of logistic regression on FMNIST when $\mu = 10^{-6}$. Relative cost is $f(\theta^t) - f(\theta^*)$.

In the i.i.d. case, for $\mu = 10^{-5}$ (Fig. 8), we see that GN-SHED, Fib-SHED, Fib-SHED+ and GIANT require a similar number of communication rounds to converge, while the amount of overall data transmitted per agent is smaller for GIANT. When $\mu = 10^{-6}$, instead, we see from Figure 9 that GIANT requires more communication rounds to converge while the same amount of information needs to be transmitted. Hence, in this case GIANT is more impacted by a lower condition number when compared to our approach. On the other hand, FedNL in both cases shows a much slower convergence speed with respect

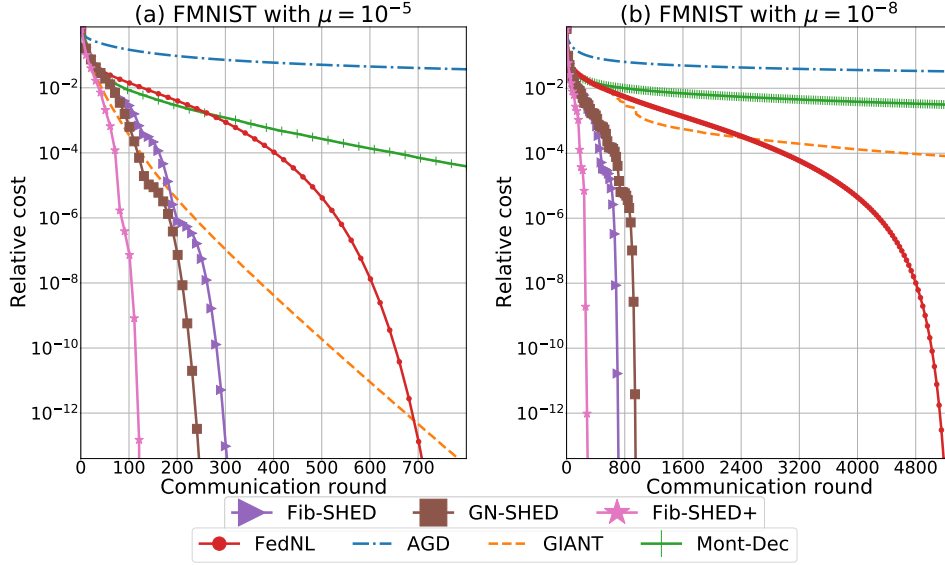


Figure 10: Performance of logistic regression on FMNIST, comparing $\mu = 10^{-5}$ and $\mu = 10^{-8}$. Relative cost is $f(\theta^t) - f(\theta^*)$.

to Fib-SHED and GN-SHED (approaches requiring the same per-iteration communication load as FedNL). Notice, for FedNL, in Figures 8-(c)-(d) and 9-(c)-(d), the impact that the transmission of the full Hessian matrices at the first round has on the overall communication load.

In the considered non i.i.d. case, the large advantage that our approach can provide with respect to the other considered algorithms is strongly evident in both data transmitted and communication rounds.

Comparing the SHED approaches against Mont-Dec we see the key role that the *incremental* strategy exploiting *outdated* second order information has on the convergence speed of our approach. Indeed, even though in the first iterations the usage of the current Hessian information provides the same performance of the SHED methods, the performance becomes largely inferior in the following rounds.

From a computational point of view, both the Mont-Dec and the FedNL approach are much heavier than SHED as they require that each agent recomputes the Hessian and SVD at each round. SHED, instead, in the more challenging case of $\mu = 10^{-6}$, requires the agents to compute the Hessian matrix only 12 times out of the 450 rounds needed for convergence. For more details on this, see Figure 11.

In Fig. 10, we show how SHED is much more resilient to ill-conditioning with respect to competing algorithms, by comparing the convergence performance when the regularization parameter is $\mu = 10^{-5}$ and $\mu = 10^{-8}$. With respect to FedNL, note how Fib-SHED worsens its performance with $\mu = 10^{-8}$ by being around 2.5 times slower compared to $\mu = 10^{-5}$, while FedNL worsens much more, being more than 8 times slower with 10^{-8} compared to $\mu = 10^{-5}$.

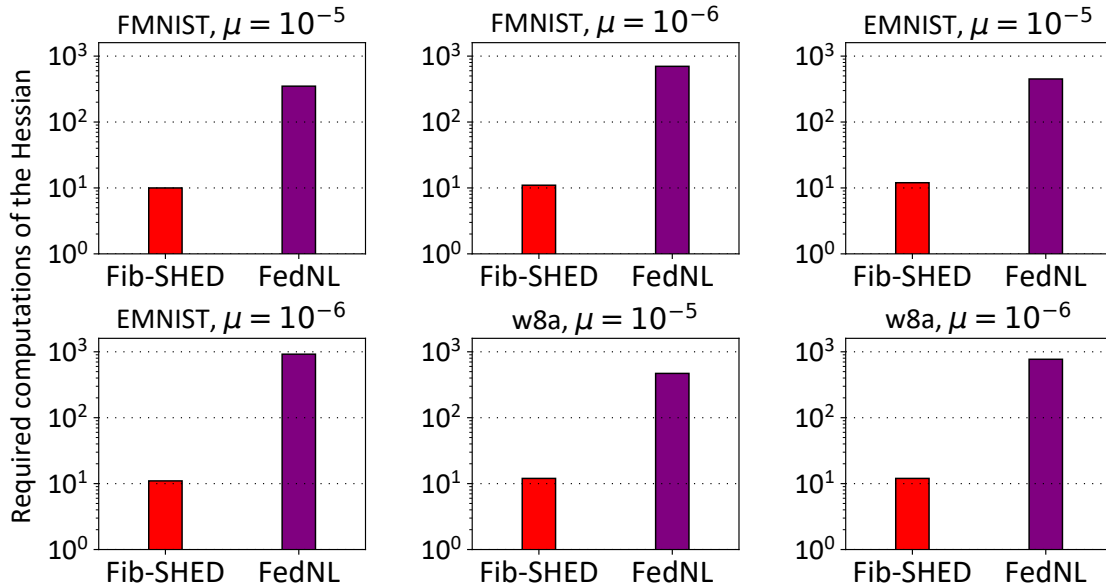


Figure 11: In this plots, we show, for three datasets (FMNIST, EMNIST and w8a), the number of times an agent is required to compute the local Hessian matrix in order for an algorithm to converge, comparing the proposed Fib-SHED and the FedNL Safaryan et al. (2021) algorithms.

6.7.3 COMPARISON ON COMPUTATIONAL COMPLEXITY

In Appendix B, we show the results obtained with the EMNIST and w8a datasets. We omit the comparison with GN-SHED given that the results are similar to the ones obtained with Fib-SHED. In the case of EMNIST, we obtain results similar to FMNIST, except that, when $\mu = 10^{-5}$, GIANT is not much impacted by the considered non i.i.d. configuration. Even if in that case GIANT seems to be the best choice, all the other results show that GIANT and related approaches based on the harmonic mean (like DONE) are strongly sensitive to non i.i.d. data distributions. With image datasets (EMNIST and FMNIST), FedNL is largely outperformed by our approach (by both Fib-SHED and Fib-SHED+), while, with the ‘w8a’ dataset, FedNL is more competitive. However, the Fib-SHED and Fib-SHED+ approaches have the very appealing feature that they require agents to compute the local Hessian matrices only *sporadically*. The FedNL approach, instead, requires that the Hessian is recomputed by agents at each round, implying a much heavier computational demand. To better illustrate and quantify this advantage, we show, in Figure 11, the number of times that an agent is required to compute the local Hessian matrix in order to obtain convergence, comparing Fib-SHED and FedNL, in the cases of the three datasets. In the case of EMNIST and FMNIST, we are showing the non i.i.d. configurations, but similar results can be obtained with the i.i.d. ones. The results show that, compared with Fib-

SHED, the number of times agents are required to compute the Hessian is always at least ten times greater for FedNL to converge.

7. Conclusions

In this work, we have proposed SHED, a Newton-type algorithm to perform FL in heterogeneous communication networks. SHED is versatile with respect to agents' (per-iteration) communication resources and operates effectively in the presence of *non i.i.d.* data distributions, outperforming state-of-the-art techniques. It achieves better performance with respect to the competing FedNL approach, while involving sporadic Hessian computations. In the case of i.i.d. data statistics, SHED is also competitive with GIANT, even though the latter may perform better under certain conditions. We stress that the key advantage of SHED lies in its robustness under any data distribution, and its effectiveness and versatility when communication resources differ across nodes and links.

Future work includes the use and extension of the algorithm for more specific scenarios and applications, like, for example, wireless networks, and also the study of new heuristics for the renewal operation in the general convex case. Furthermore, future research directions may deal with compression techniques for the Hessian eigenvectors, as well as the development of heuristic algorithms combining different second-order methods, like FedNL and SHED. Lastly, the spectral characteristics of the data could also be exploited to tailor the proposed algorithm to specific FL problems, leading to further benefits in terms of convergence speed.

Acknowledgments

This work has been supported, in part, by the Italian Ministry of Education, University and Research, through the PRIN project no. 2017NS9FEY entitled "Realtime Control of 5G Wireless Networks: Taming the Complexity of Future Transmission and Computation Challenges".

Appendix A.

Proof of Theorem 8

First, we need to prove the following Lemma:

Lemma 11 *If $\|\mathbf{g}_t\| > \omega > 0$, for $\hat{\mathbf{H}}_t$ defined in (26), $\mathbf{p}_t = \hat{\mathbf{H}}_t^{-1} \mathbf{g}_t$ there are $\gamma_t, \eta_t > 0$ such that*

$$f(\boldsymbol{\theta}^t - \eta_t \mathbf{p}_t) \leq f(\boldsymbol{\theta}^t) - \gamma_t, \quad (39)$$

in particular, for a backtracking line search with parameters $\alpha \in (0, 0.5), \beta \in (0, 1)$, it holds:

$$\gamma_t = \alpha \beta \frac{\bar{\rho}_t}{K^2} \omega^2 \quad (40)$$

Proof The proof is the same as the one provided in Boyd and Vandenberghe (2004) for the damped Newton phase (page 489-490), with the difference that the "Newton decrement",

that we denote by σ_t , here is $\sigma_t^2 := \mathbf{g}_t^T \mathbf{p}_t = \mathbf{g}_t^T \hat{\mathbf{H}}_t^{-1} \mathbf{g}_t = \mathbf{p}_t^T \hat{\mathbf{H}}_t \mathbf{p}_t$. Furthermore, the property $\hat{\mathbf{H}}_t \geq \bar{\rho}_t \mathbf{I}$, $\forall t$ is used in place of strong convexity. \blacksquare

Note that, because of Assumption 1, it always holds that $\rho_t^{(i)} > 0$, $\forall i, \forall t$, and this implies $\bar{\rho}_t > 0, \forall t$. When $\bar{\rho}_t > 0, \forall t$, Lemma 11 implies $\|\mathbf{g}_t\| \rightarrow 0$. Indeed, if not, there would be some $\epsilon > 0$ such that $\|\mathbf{g}_t\| > \epsilon$, $\forall t$. But then (39) immediately implies that $f(\boldsymbol{\theta}^t) \rightarrow -\infty$, that contradicts the strong convexity hypothesis. By strong convexity and differentiability of f , $g(\boldsymbol{\theta}) = \nabla f(\boldsymbol{\theta}) = 0 \implies \boldsymbol{\theta} = \boldsymbol{\theta}^*$.

Proof of Theorem 10

1) We first need the following Lemma:

Lemma 12 *Let $\bar{\kappa} = \sum_{i=1}^M \kappa_i$, with κ_i the strong convexity constant of the cost $f^{(i)}$ of agent i , let K be the smoothness constant of f and $M(t) = \max\{\|\boldsymbol{\theta}^t - \boldsymbol{\theta}^*\|, \|\boldsymbol{\theta}^{k_t} - \boldsymbol{\theta}^*\|\}$. Applying Algorithm 4, if*

$$3\bar{\kappa}(M(t) + \|\boldsymbol{\theta}^t - \boldsymbol{\theta}^*\|) + K\|\boldsymbol{\theta}^t - \boldsymbol{\theta}^*\| \leq \frac{3\bar{\kappa}^2}{L}(1 - 2\alpha), \quad (41)$$

then, for any $\alpha \in (0, 1/2)$, the backtracking algorithm (2) chooses $\eta_t = 1$.

Proof [Sketch of proof] The proof uses a procedure similar to the one used in Boyd and Vandenberghe (2004), page 490-491 to prove the beginning of the quadratically convergent phase in the centralized Newton method. Then, leveraging Lipschitz continuity and the fact that, thanks to the choice $\rho_t^{(i)} = \lambda_{q_t}^{(i)}$, it is $\hat{\mathbf{H}}_t \geq \mathbf{H}(\boldsymbol{\theta}^{k_t})$, the result is derived. For the complete proof, see the Proof of Lemma 12 at the end of this Appendix. \blacksquare

Let condition (41) be satisfied. Then, if

$$(3/2)L\|\boldsymbol{\theta}^t - \boldsymbol{\theta}^*\| + LM(t) \leq \bar{\kappa}, \quad (42)$$

the convergence of SHED is at least linear. Indeed, if (41) is satisfied, then, from Lemma 12, the step size is $\eta_t = 1$ and the convergence bound (see Theorem 9) becomes $\|\boldsymbol{\theta}^{t+1} - \boldsymbol{\theta}^*\| \leq c_t \|\boldsymbol{\theta}^t - \boldsymbol{\theta}^*\|$, with

$$\begin{aligned} c_t &= \left(1 - \frac{\bar{\lambda}_{n,t}}{\bar{\rho}_t} + \frac{L}{\bar{\rho}_t} \|\boldsymbol{\theta}^t - \boldsymbol{\theta}^{k_t}\| + \frac{L}{2\bar{\rho}_t} \|\boldsymbol{\theta}^t - \boldsymbol{\theta}^*\|\right) \\ &\leq \left(1 - \frac{\bar{\lambda}_{n,t}}{\bar{\rho}_t} + \frac{L}{\bar{\rho}_t} \|\boldsymbol{\theta}^{k_t} - \boldsymbol{\theta}^*\| + \frac{3L}{2\bar{\rho}_t} \|\boldsymbol{\theta}^t - \boldsymbol{\theta}^*\|\right) \end{aligned} \quad (43)$$

and it is easy to see that condition (42) implies that $c_t < 1$ and thus we get a contraction in $\|\boldsymbol{\theta}^t - \boldsymbol{\theta}^*\|$. Furthermore, when conditions (41) and (42) are both satisfied at some iteration \bar{t} , they are then satisfied for all $t \geq \bar{t}$ and thus $c_t < 1$ for all $t \geq \bar{t}$. Indeed, $c_t < 1$ implies that $\|\boldsymbol{\theta}^{t+1} - \boldsymbol{\theta}^*\| < \|\boldsymbol{\theta}^t - \boldsymbol{\theta}^*\|$ and $M(t+1) \leq M(t)$ because either $k_{t+1} = k_t$ or $k_{t+1} = t+1$. Note that Assumption 3 is needed to guarantee that (41) and (42) are eventually satisfied.

2) From 1), we can write $\|\boldsymbol{\theta}^t - \boldsymbol{\theta}^*\| \leq Ca^t$ for some $a \in (0, 1)$ and some $C > 0$. Considering $t \geq \bar{t}$, with \bar{t} the first iteration for which both conditions (41) and (42) are satisfied, we consider c_t as in (43), and let $T = t - k_t$

$$\begin{aligned} c_t &\leq 1 - \frac{\bar{\lambda}_{n,t}}{\bar{\rho}_t} + \frac{L}{\bar{\rho}_t} \|\boldsymbol{\theta}^{k_t} - \boldsymbol{\theta}^*\| + \frac{3L}{2\bar{\rho}_t} \|\boldsymbol{\theta}^t - \boldsymbol{\theta}^*\| \\ &\leq 1 - \frac{\bar{\lambda}_{n,t}}{\bar{\rho}_t} + \frac{L}{\bar{\rho}_t} C_1 a_*^{t-T} + \frac{3L}{2\bar{\rho}_t} C_2 a_*^t \\ &= 1 - \frac{\bar{\lambda}_{n,t}}{\bar{\rho}_t} + Ba_*^t, \end{aligned} \quad (44)$$

where $B = \frac{L}{\bar{\rho}_t} C_1 a_*^{-T} + \frac{3L}{2\bar{\rho}_t} C_2$, and C_1, C_2 are some bounded positive constants. For any iteration t , we can write $\|\boldsymbol{\theta}^{t+1} - \boldsymbol{\theta}^*\| \leq \bar{c}_t \|\boldsymbol{\theta}^t - \boldsymbol{\theta}^*\|$ for some \bar{c}_t that could also be greater than one, if $t < \bar{t}$, but it is easy to see that \bar{c}_t is always bounded. Now, we consider $\bar{a} := \limsup_t (\prod_{k=1}^t \bar{c}_k)^{1/t}$. It is straightforward to see that, as in the least squares case, it is $a_* \leq \bar{a}$. We can write $\log \bar{a} = \limsup_t \frac{1}{t} (\sum_{k=\bar{t}+1}^t \log c_k)$. We get

$$\begin{aligned} \log \bar{a} &\leq \limsup_t \frac{1}{t} \left(\sum_{k=\bar{t}+1}^t \log c_k \right) \\ &\leq \limsup_t \frac{1}{t} \sum_{k=\bar{t}+1}^t \log \left(1 - \frac{\bar{\lambda}_{n,k}}{\bar{\rho}_k} + Ba_*^k \right) \\ &= \limsup_t \frac{1}{t} \sum_{k=\bar{t}+1}^t \log \left(1 - \frac{\bar{\lambda}_{n,k}}{\bar{\rho}_k} \right) + \log \left(1 + \frac{Ba_*^k}{1 - \frac{\bar{\lambda}_{n,k}}{\bar{\rho}_k}} \right). \end{aligned}$$

We see that the last term is

$$\log \left(1 + \frac{Ba_*^k}{1 - \frac{\bar{\lambda}_{n,k}}{\bar{\rho}_k}} \right) \leq \frac{Ba_*^k}{1 - \frac{\bar{\lambda}_{n,k}}{\bar{\rho}_k}} \leq \bar{B} a_*^k$$

that comes from the identity $\log(1+x) \leq x$, and where $\bar{B} = \max_k \frac{1}{1 - \frac{\bar{\lambda}_{n,k}}{\bar{\rho}_k}}$, bounded because $|\mathcal{X}_t = 0|$, $\forall t$, and thus $\bar{\rho}_k > \bar{\lambda}_{n,k}, \forall k$. Now, we see that

$$\limsup_t \frac{1}{t} \sum_{k=1}^t \bar{B} a_*^k = \limsup_t \frac{1}{t} \bar{B} \left(\frac{1 - a_*^{t+1}}{1 - a_*} - 1 \right) = 0.$$

Hence, we get, using also the finiteness of \bar{t} ,

$$\log \bar{a} = \limsup_t \frac{1}{t} \sum_{k=1}^t \log \left(1 - \frac{\bar{\lambda}_{n,k}}{\bar{\rho}_k} \right). \quad (45)$$

Now we use local Lipschitz continuity (Assumption 1) to conclude the proof. Lipschitz continuity of $f^{(i)}(\boldsymbol{\theta})$ implies that, for any $k \in \{1, \dots, n\}$, $|\lambda_k^{(i)}(\boldsymbol{\theta}) - \lambda_k^{(i)}(\boldsymbol{\theta}^*)| \leq \bar{L} \|\boldsymbol{\theta} - \boldsymbol{\theta}^*\|$, which in turn implies $\lambda_k^{(i)}(\boldsymbol{\theta}) \geq \lambda_k^{(i)}(\boldsymbol{\theta}^*) - \bar{L} \|\boldsymbol{\theta} - \boldsymbol{\theta}^*\|$ and $\lambda_k^{(i)}(\boldsymbol{\theta}) \leq \lambda_k^{(i)}(\boldsymbol{\theta}^*) + \bar{L} \|\boldsymbol{\theta} - \boldsymbol{\theta}^*\|$. For a proof of this result, see also Bisgard (2020), page 116, Theorem 4.25. It follows that

$$\begin{aligned}
 \log \bar{a} &\leq \limsup_t \frac{1}{t} \sum_{k=1}^t \log \left(1 - \frac{\bar{\lambda}_n^o - \bar{L} \|\boldsymbol{\theta}^{k_t} - \boldsymbol{\theta}^*\|}{\bar{\rho}_k^o + \bar{L} \|\boldsymbol{\theta}^{k_t} - \boldsymbol{\theta}^*\|} \right) \\
 &\stackrel{(1)}{=} \limsup_t \frac{1}{t} \sum_{k=1}^t \log \left(1 - \frac{\bar{\lambda}_n^o}{\bar{\rho}_k^o + \bar{L} \|\boldsymbol{\theta}^{k_t} - \boldsymbol{\theta}^*\|} \right) \\
 &= \limsup_t \frac{1}{t} \sum_{k=1}^t \log \left(\frac{\bar{\rho}_k^o - \bar{\lambda}_n^o + \bar{L} \|\boldsymbol{\theta}^{k_t} - \boldsymbol{\theta}^*\|}{\bar{\rho}_k^o + \bar{L} \|\boldsymbol{\theta}^{k_t} - \boldsymbol{\theta}^*\|} \right) \\
 &\leq \limsup_t \frac{1}{t} \sum_{k=1}^t \log \left(1 - \frac{\bar{\lambda}_n^o}{\bar{\rho}_k^o} + \frac{\bar{L} \|\boldsymbol{\theta}^{k_t} - \boldsymbol{\theta}^*\|}{\bar{\rho}_k^o} \right) \\
 &\stackrel{(2)}{=} \limsup_t \frac{1}{t} \sum_{k=1}^t \log \left(1 - \frac{\bar{\lambda}_n^o}{\bar{\rho}_k^o} \right)
 \end{aligned}$$

where equalities (1) and (2) follow from calculations equivalent to the ones used to obtain (45).

3) Consider c_t as it was defined and bounded in (44), $C_3 > 0$ a constant such that $\log c_k \leq C_3$, $\forall k$, and such that $\log B \leq C_3$. Let \bar{a} be defined as before. Let $a \in (0, 1)$. We have

$$\begin{aligned}
 \log \bar{a} &= \limsup_t \frac{1}{t} \sum_{k=1}^t \log c_k \\
 &\leq \limsup_t \frac{1}{t} \sum_{k=1}^t \log \left(1 - \frac{\bar{\lambda}_{n,k}}{\bar{\rho}_k} + Ba^k \right) \\
 &= \limsup_t \frac{1}{t} \left(\sum_{k \notin \mathcal{X}_t} \log c_k + \sum_{k \in \mathcal{X}_t} \log Ba^k \right) \tag{46} \\
 &\leq 2C_3 + \limsup_t \frac{1}{t} \log a \sum_{k \in \mathcal{X}_t} k \\
 &\leq 2C_3 + \limsup_t \frac{1}{t} \log a C_4 |\mathcal{X}_t|^2 \\
 &= 2C_3 + \limsup_t \log a C_4 h(t)^2 = -\infty
 \end{aligned}$$

where $C_4 > 0$ is some positive constant and the last equality follows because $\log a < 0$ and $\lim_t h(t) = \infty$. We see that $0 \leq a_* \leq \bar{a} \leq 0$, which implies $a_* = 0$.

Proof of Lemma 12

The following proof is similar to the proof for the beginning of the quadratically convergent phase in centralized Newton method by Boyd and Vandenberghe (2004), page 490-491. We start with some definitions: at iteration t , let $f(\boldsymbol{\theta}^t)$, $\mathbf{g}_t = \nabla f(\boldsymbol{\theta}^t)$, $\mathbf{H}_t = \nabla^2 f(\boldsymbol{\theta}^t)$ be the cost, the gradient and the Hessian, respectively, computed at $\boldsymbol{\theta}^t$. Let $\mathbf{H}_{k_t} = \nabla^2 f(\boldsymbol{\theta}^{k_t})$ be the Hessian at $\boldsymbol{\theta}^{k_t}$, and $\hat{\mathbf{H}}_t$ the global Hessian approximation of Algorithm 4. Let the NT

descent direction be $\mathbf{p}_t = \hat{\mathbf{H}}_t^{-1} \mathbf{g}_t$. Define

$$\begin{aligned}
 \bar{\sigma}_t^2 &:= \mathbf{p}_t^T \mathbf{g}_t = \mathbf{g}_t^T \hat{\mathbf{H}}_t^{-1} \mathbf{g}_t, \\
 \sigma_t^2 &:= \mathbf{p}_t^T \nabla^2 f(\boldsymbol{\theta}^t) \mathbf{p}_t = \mathbf{p}_t^T \mathbf{H}_t \mathbf{p}_t, \\
 \tilde{f}(\eta) &:= f(\boldsymbol{\theta}^t - \eta \mathbf{p}_t), \quad \tilde{f}(0) = f(\boldsymbol{\theta}^t), \\
 \tilde{f}'(\eta) &:= \frac{\partial \tilde{f}(\eta)}{\partial \eta} = -\nabla f(\boldsymbol{\theta}^t - \eta \mathbf{p}_t)^T \mathbf{p}_t, \\
 \tilde{f}''(\eta) &:= \frac{\partial^2 \tilde{f}(\eta)}{\partial \eta^2} = \mathbf{p}_t^T \nabla^2 f(\boldsymbol{\theta}^t - \eta \mathbf{p}_t) \mathbf{p}_t.
 \end{aligned} \tag{47}$$

Note that

$$\begin{aligned}
 \tilde{f}'(0) &= -\mathbf{g}_t^T \mathbf{p}_t = -\bar{\sigma}_t^2, \\
 \tilde{f}''(0) &= \mathbf{p}_t^T \mathbf{H}_t \mathbf{p}_t = \sigma_t^2.
 \end{aligned} \tag{48}$$

Note that $\hat{\mathbf{H}}_t \geq \bar{\kappa}$, $\forall t$. Thanks to L -Lipschitz continuity, it holds that $\|\nabla^2 f(\boldsymbol{\theta}^t - \eta \mathbf{p}_t) - \nabla^2 f(\boldsymbol{\theta}^t)\| \leq \eta L \|\mathbf{p}_t\|$ and we have that

$$\begin{aligned}
 |\tilde{f}''(\eta) - \tilde{f}''(0)| &= \mathbf{p}_t^T (\nabla^2 f(\boldsymbol{\theta}^t - \eta \mathbf{p}_t) - \nabla^2 f(\boldsymbol{\theta}^t)) \mathbf{p}_t \\
 &\leq \eta L \|\mathbf{p}_t\|^3 \leq \eta L \frac{\bar{\sigma}_t^3(\boldsymbol{\theta}^t)}{\bar{\kappa}^{3/2}}
 \end{aligned} \tag{49}$$

where the last inequality holds because $\bar{\kappa} \|\mathbf{p}_t\|^2 \leq \mathbf{p}_t^T \hat{\mathbf{H}}_t \mathbf{p}_t = \bar{\sigma}_t^2$. From (49) it follows that

$$\tilde{f}''(\eta) \leq \tilde{f}''(0) + \eta L \frac{\bar{\sigma}_t^3(\boldsymbol{\theta}^t)}{\bar{\kappa}^{3/2}} = \sigma_t^2 + \eta L \frac{\bar{\sigma}_t^3(\boldsymbol{\theta}^t)}{\bar{\kappa}^{3/2}}. \tag{50}$$

Similarly to Boyd and Vandenberghe (2004), page 490-491, we can now integrate both sides of the inequality getting

$$\tilde{f}'(\eta) \leq \tilde{f}'(0) + \eta \sigma_t^2 + \frac{\eta^2}{2} L \frac{\bar{\sigma}_t^3}{\bar{\kappa}^{3/2}} = -\bar{\sigma}_t^2 + \eta \sigma_t^2 + \frac{\eta^2}{2} L \frac{\bar{\sigma}_t^3}{\bar{\kappa}^{3/2}}.$$

By integrating again both sides of the inequality, we get, recalling that $\tilde{f}(0) = f(\boldsymbol{\theta}^t)$,

$$\tilde{f}(\eta) = f(\boldsymbol{\theta}^t - \eta \mathbf{p}_t) \leq f(\boldsymbol{\theta}^t) - \eta \bar{\sigma}_t^2 + \frac{\eta^2}{2} \sigma_t^2 + \frac{\eta^3}{6} L \frac{\bar{\sigma}_t^3}{\bar{\kappa}^{3/2}}. \tag{51}$$

Now, recalling $\mathbf{H}(\boldsymbol{\theta}^{k_t}) \leq \hat{\mathbf{H}}_t$, we get that

$$\begin{aligned}
 \sigma_t^2 &= \mathbf{p}_t^T \mathbf{H}_t \mathbf{p}_t = \mathbf{p}_t^T (\mathbf{H}_{k_t} + \mathbf{H}_t - \mathbf{H}_{k_t}) \mathbf{p}_t \\
 &= \mathbf{p}_t^T \mathbf{H}_{k_t} \mathbf{p}_t + \mathbf{p}_t^T (\mathbf{H}_t - \mathbf{H}_{k_t}) \mathbf{p}_t \\
 &\leq \mathbf{p}_t^T \hat{\mathbf{H}}_t \mathbf{p}_t + L \|\mathbf{p}_t\|^2 \|\boldsymbol{\theta}^t - \boldsymbol{\theta}^{k_t}\| \leq \bar{\sigma}_t^2 + \frac{L \bar{\sigma}_t^2}{\bar{\kappa}} \|\boldsymbol{\theta}^t - \boldsymbol{\theta}^{k_t}\|,
 \end{aligned} \tag{52}$$

where we have used Lipschitz continuity, and the fact that $\mathbf{p}_t^T \hat{\mathbf{H}}_t \mathbf{p}_t = \bar{\sigma}_t^2$ and $\bar{\kappa} \|\mathbf{p}_t\|^2 \leq \bar{\sigma}_t^2$. Next, setting $\eta = 1$ and plugging (52) in (51), we get

$$\begin{aligned}
 f(\boldsymbol{\theta}^t - \mathbf{p}_t) &\leq f(\boldsymbol{\theta}^t) - \bar{\sigma}_t^2 + \frac{\sigma_t^2}{2} + \frac{L}{6} \frac{\bar{\sigma}_t^3}{\bar{\kappa}^{3/2}} \\
 &\leq f(\boldsymbol{\theta}^t) - \frac{\bar{\sigma}_t^2}{2} + \frac{L\bar{\sigma}_t^2}{2\bar{\kappa}} \|\boldsymbol{\theta}^t - \boldsymbol{\theta}^{k_t}\| + \frac{L}{6} \frac{\bar{\sigma}_t^3}{\bar{\kappa}^{3/2}} \\
 &\leq f(\boldsymbol{\theta}^t) - \bar{\sigma}_t^2 \left(\frac{1}{2} - \frac{L}{2\bar{\kappa}} \|\boldsymbol{\theta}^t - \boldsymbol{\theta}^{k_t}\| - \frac{L}{6} \frac{\bar{\sigma}_t}{\bar{\kappa}^{3/2}} \right) \\
 &= f(\boldsymbol{\theta}^t) - \mathbf{p}_t^T \mathbf{g}_t \left(\frac{1}{2} - \frac{L}{2\bar{\kappa}} \|\boldsymbol{\theta}^t - \boldsymbol{\theta}^{k_t}\| - \frac{L}{6} \frac{\bar{\sigma}_t}{\bar{\kappa}^{3/2}} \right).
 \end{aligned} \tag{53}$$

In order for (53) to satisfy the Armijo-Goldstein condition (18) for any parameter $\alpha \in (0, 1/2)$ we see that

$$\frac{1}{2} - \frac{L}{2\bar{\kappa}} \|\boldsymbol{\theta}^t - \boldsymbol{\theta}^{k_t}\| - \frac{L}{6} \frac{\bar{\sigma}_t}{\bar{\kappa}^{3/2}} \geq \alpha \tag{54}$$

provides a sufficient condition. The above inequality can be written as

$$3\bar{\kappa} \|\boldsymbol{\theta}^t - \boldsymbol{\theta}^{k_t}\| + \bar{\kappa}^{1/2} \bar{\sigma}_t \leq \frac{3\bar{\kappa}^2}{L} (1 - 2\alpha). \tag{55}$$

We have that $\bar{\sigma}_t^2 = \mathbf{g}_t^T \hat{\mathbf{H}}^{-1} \mathbf{g}_t \leq \|\mathbf{g}_t\|^2 / \bar{\kappa}$, which implies $\bar{\kappa}^{1/2} \|\sigma_t\| \leq \|\mathbf{g}_t\|$. Furthermore, by triangular inequality, we have $\|\boldsymbol{\theta}^t - \boldsymbol{\theta}^{k_t}\| \leq \|\boldsymbol{\theta}^t - \boldsymbol{\theta}^*\| + \|\boldsymbol{\theta}^{k_t} - \boldsymbol{\theta}^*\|$. Therefore, we see that if

$$3\bar{\kappa} (\|\boldsymbol{\theta}^t - \boldsymbol{\theta}^*\| + \|\boldsymbol{\theta}^{k_t} - \boldsymbol{\theta}^*\|) + \|\mathbf{g}_t\| \leq \frac{3\bar{\kappa}^2}{L} (1 - 2\alpha), \tag{56}$$

then the Armijo-Goldstein condition is satisfied and $\eta = 1$ is chosen by the backtracking algorithm, proving the Lemma. Indeed, by K -smoothness of the cost function (see Assumption 1) we have $\|\mathbf{g}_t\| \leq K \|\boldsymbol{\theta}^t - \boldsymbol{\theta}^*\|$ and so the condition of the Lemma implies (56).

Appendix B.

Results on EMNIST digits and w8a

In this appendix, we include the results on the EMNIST digits and ‘w8a’ datasets when comparing the different algorithms. We show results for two values of the regularization parameter μ , specifically $\mu = 10^{-5}$ and $\mu = 10^{-6}$, in Figure 12 and 13, respectively. The results obtained on the EMNIST digits dataset confirm the results that were obtained with FMNIST, with the difference that in the case $\mu = 10^{-5}$, GIANT is not much impacted by the considered non i.i.d. configuration. The results obtained with the ‘w8a’ dataset show that, while GIANT performance is largely degraded because of the non i.i.d. configuration, also in this case Fib-SHED and Fib-SHED+ significantly outperform FedNL in both communication rounds and communication load required for convergence.

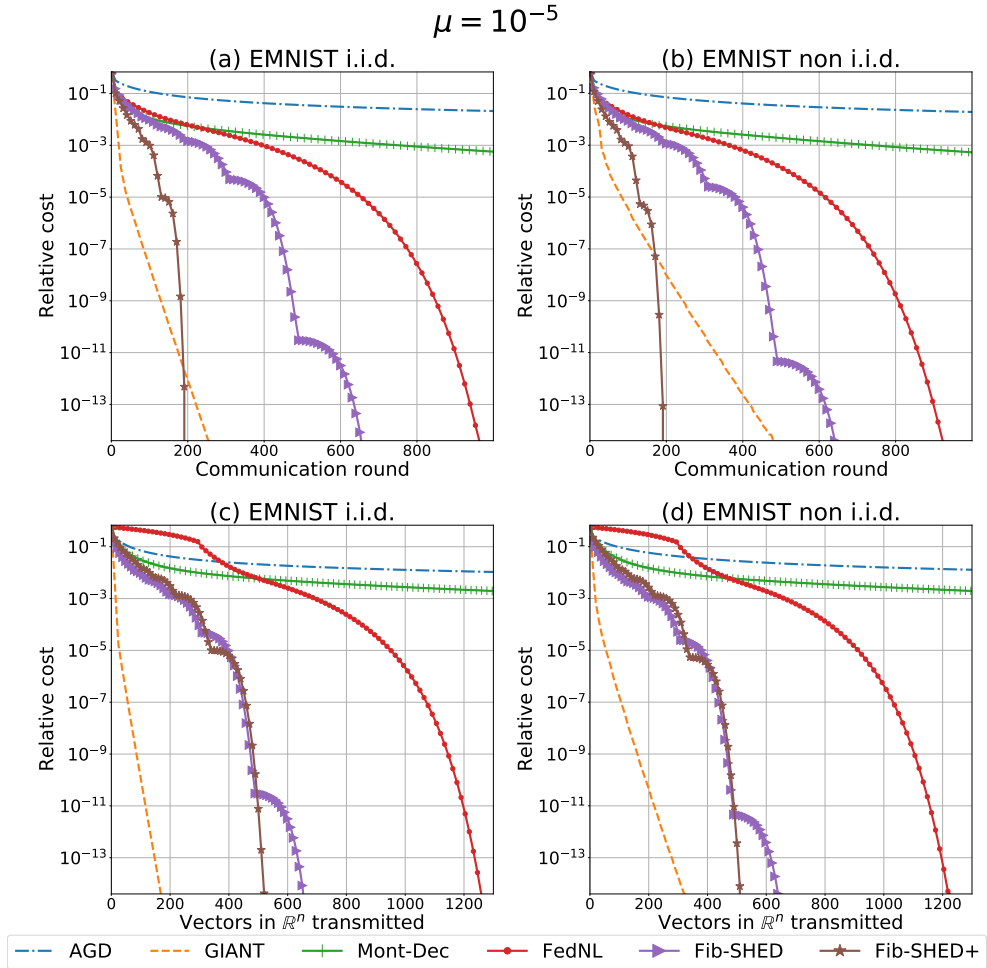


Figure 12: Performance comparison of logistic regression on EMNIST when $\mu = 10^{-5}$. Relative cost is $f(\theta^t) - f(\theta^*)$.

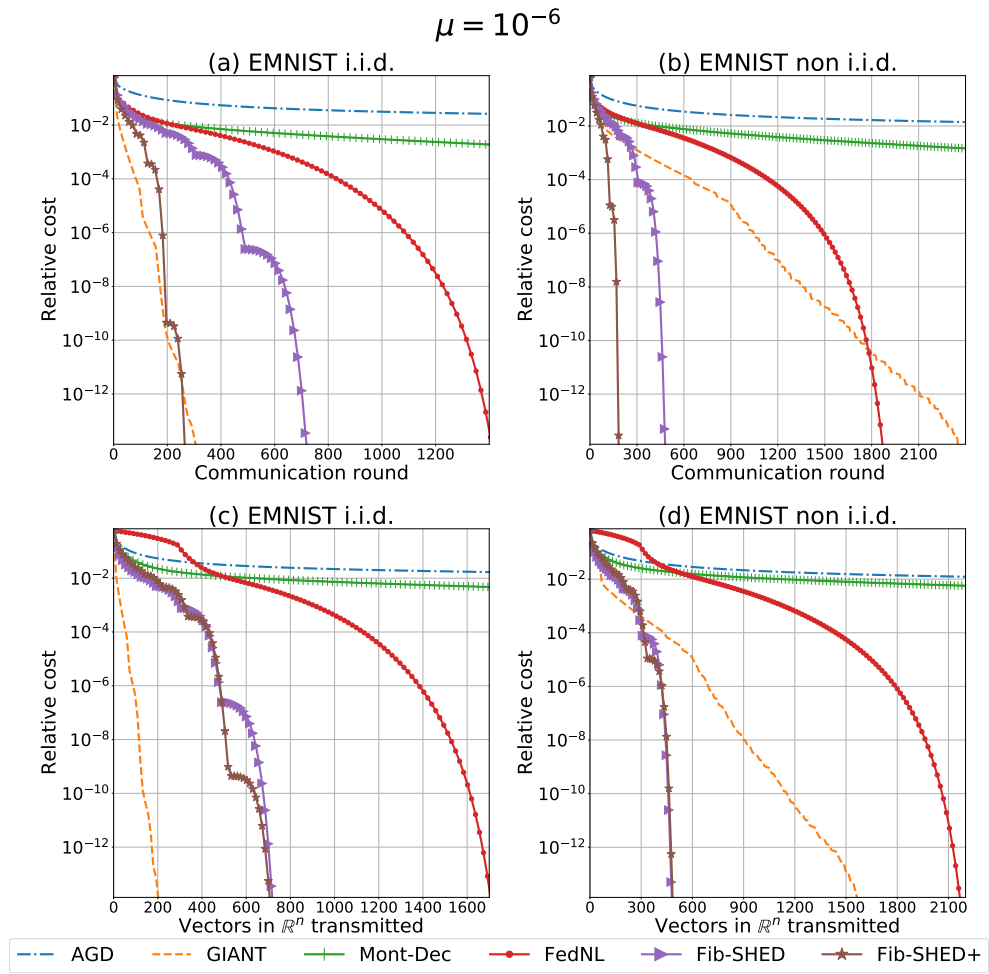


Figure 13: Performance comparison of logistic regression on EMNIST when $\mu = 10^{-6}$. Relative cost is $f(\theta^t) - f(\theta^*)$.

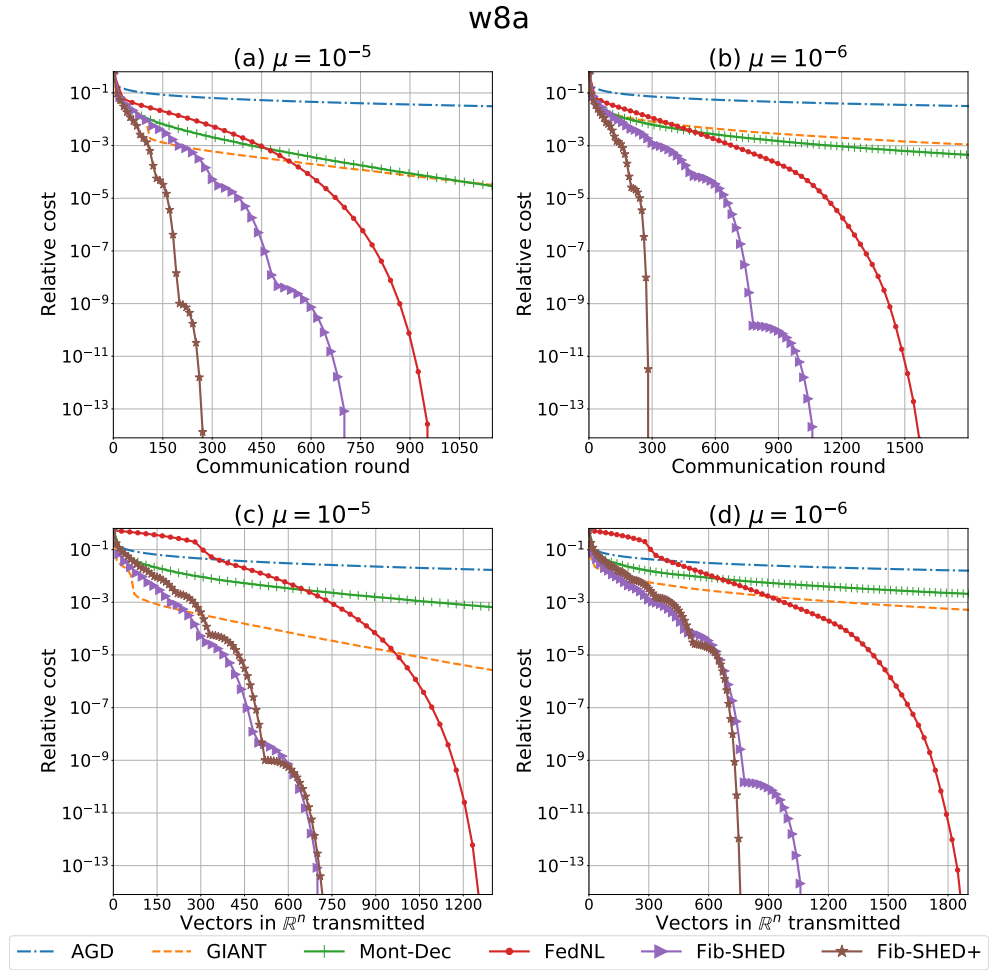


Figure 14: Performance comparison of logistic regression on w8a when $\mu = 10^{-5}$ and $\mu = 10^{-6}$. Relative cost is $f(\theta^t) - f(\theta^*)$.

References

- Artem Agafonov, Dmitry Kamzolov, Rachael Tappenden, Alexander Gasnikov, and Martin Takáč. Flecs: A federated learning second-order framework via compression and sketching. *arXiv preprint arXiv:2206.02009*, 2022.
- Foivos Alimisis, Peter Davies, and Dan Alistarh. Communication-efficient distributed optimization with quantized preconditioners. In Marina Meila and Tong Zhang, editors, *Proceedings of the 38th International Conference on Machine Learning*, volume 139 of *Proceedings of Machine Learning Research*, pages 196–206. PMLR, 18–24 Jul 2021.
- Mohammad Mohammadi Amiri and Deniz Gündüz. Federated learning over wireless fading channels. *IEEE Transactions on Wireless Communications*, 19(5):3546–3557, 2020.
- Thierry Bertin-Mahieux, Daniel P.W. Ellis, Brian Whitman, and Paul Lamere. The million song dataset. In *Proceedings of the 12th International Conference on Music Information Retrieval (ISMIR 2011)*, 2011.
- James Bisgard. *Analysis and Linear Algebra: The Singular Value Decomposition and Applications*, volume 94. American Mathematical Soc., 2020.
- Stephen Boyd and Lieven Vandenberghe. *Convex optimization*. Cambridge university press, 2004.
- Chih-Chung Chang and Chih-Jen Lin. LIBSVM: A library for support vector machines. *ACM Transactions on Intelligent Systems and Technology*, 2:27:1–27:27, 2011. Software available at <http://www.csie.ntu.edu.tw/~cjlin/libsvm>.
- Mingzhe Chen, Zhaohui Yang, Walid Saad, Changchuan Yin, H Vincent Poor, and Shuguang Cui. A joint learning and communications framework for federated learning over wireless networks. *IEEE Transactions on Wireless Communications*, 20(1):269–283, 2020.
- Tianyi Chen, Georgios Giannakis, Tao Sun, and Wotao Yin. Lag: Lazily aggregated gradient for communication-efficient distributed learning. *Advances in neural information processing systems*, 2018.
- Gregory Cohen, Saeed Afshar, Jonathan Tanson, and André van Schaik. Emnist: Extending mnist to handwritten letters. In *2017 International Joint Conference on Neural Networks (IJCNN)*, pages 2921–2926, 2017. doi: 10.1109/IJCNN.2017.7966217.
- Rixon Crane and Fred Roosta. DINGO: Distributed newton-type method for gradient-norm optimization. *Advances in Neural Information Processing Systems*, 32, 2019.
- Adam Czornik, Aleksander Nawrat, Michal Niezabitowski, and Aneta Szyda. On the lyapunov and bohl exponent of time-varying discrete linear system. In *2012 20th Mediterranean Conference on Control Automation (MED)*, 2012.
- Michał Dereziński and Michael W. Mahoney. Distributed estimation of the inverse hessian by determinantal averaging. In *Proceedings of the 33rd International Conference on Neural Information Processing Systems*, Red Hook, NY, USA, 2019. Curran Associates Inc.

- Dheeru Dua and Casey Graff. UCI machine learning repository, 2017. URL <http://archive.ics.uci.edu/ml>.
- Anis Elgabli, Chaouki Ben Issaid, Amrit Singh Bedi, Ketan Rajawat, Mehdi Bennis, and Vaneet Aggarwal. Fednew: A communication-efficient and privacy-preserving newton-type method for federated learning. In *International Conference on Machine Learning*, pages 5861–5877. PMLR, 2022.
- Murat A Erdogdu and Andrea Montanari. Convergence rates of sub-sampled newton methods. *Advances in Neural Information Processing Systems*, 28, 2015.
- Kelwin Fernandes, Pedro Vinagre, and Paulo Cortez. A proactive intelligent decision support system for predicting the popularity of online news. In *Portuguese conference on artificial intelligence*. Springer, 2015.
- Vipul Gupta, Avishek Ghosh, Michał Dereziński, Rajiv Khanna, Kannan Ramchandran, and Michael W Mahoney. LocalNewton: Reducing communication rounds for distributed learning. In *Uncertainty in Artificial Intelligence*. PMLR, 2021.
- Andrew Hard, Kanishka Rao, Rajiv Mathews, Swaroop Ramaswamy, Françoise Beaufays, Sean Augenstein, Hubert Eichner, Chloé Kiddon, and Daniel Ramage. Federated learning for mobile keyboard prediction. *arXiv preprint arXiv:1811.03604*, 2018.
- Li Huang, Yifeng Yin, Zeng Fu, Shifa Zhang, Hao Deng, and Dianbo Liu. Loadaboost: Loss-based adaboost federated machine learning with reduced computational complexity on iid and non-iid intensive care data. *PLOS ONE*, 15(4):1–16, 04 2020.
- Rustem Islamov, Xun Qian, and Peter Richtárik. Distributed second order methods with fast rates and compressed communication. In *Proceedings of the 38th International Conference on Machine Learning*. PMLR, 2021.
- Eunjeong Jeong, Seungeun Oh, Hyesung Kim, Jihong Park, Mehdi Bennis, and Seong-Lyun Kim. Communication-efficient on-device machine learning: Federated distillation and augmentation under non-iid private data. *arXiv preprint arXiv:1811.11479*, 2018.
- Peter Kairouz, H. Brendan McMahan, et al. Advances and open problems in federated learning. *Foundations and Trends® in Machine Learning*, 14(1-2):1–210, 2021.
- Sai Praneeth Karimireddy, Satyen Kale, Mehryar Mohri, Sashank Reddi, Sebastian Stich, and Ananda Theertha Suresh. SCAFFOLD: Stochastic controlled averaging for federated learning. In *Proceedings of the 37th International Conference on Machine Learning*. PMLR, 2020.
- Tian Li, Anit Kumar Sahu, Ameet Talwalkar, and Virginia Smith. Federated learning: Challenges, methods, and future directions. *IEEE Signal Processing Magazine*, 37(3): 50–60, 2020a.
- Tian Li, Anit Kumar Sahu, Manzil Zaheer, Maziar Sanjabi, Ameet Talwalkar, and Virginia Smith. Federated optimization in heterogeneous networks. In I. Dhillon, D. Papailiopoulos, and V. Sze, editors, *Proceedings of Machine Learning and Systems*, 2020b.

- Dong C Liu and Jorge Nocedal. On the limited memory BFGS method for large scale optimization. *Mathematical programming*, 45(1):503–528, 1989.
- Yaqiong Liu, Mugen Peng, Guochu Shou, Yudong Chen, and Siyu Chen. Toward Edge Intelligence: Multiaccess Edge Computing for 5G and Internet of Things. *IEEE Internet of Things Journal*, 7, 2020.
- Yi Liu, Yuanshao Zhu, and JQ James. Resource-constrained federated learning with heterogeneous data: Formulation and analysis. *IEEE Transactions on Network Science and Engineering*, 2021.
- Aleksandr Mikhailovich Lyapunov. The general problem of the stability of motion. *International journal of control*, 55(3):531–534, 1992.
- H. B. McMahan, Eider Moore, D. Ramage, S. Hampson, and B. A. Y. Arcas. Communication-efficient learning of deep networks from decentralized data. In *AISTATS*, 2017.
- Tuan Dung Nguyen, Amir R. Balef, Canh T. Dinh, Nguyen H. Tran, Duy T. Ngo, Tuan Anh Le, and Phuong L. Vo. Accelerating federated edge learning. *IEEE Communications Letters*, 25(10):3282–3286, 2021.
- Francesco Pase, Marco Giordani, and Michele Zorzi. On the convergence time of federated learning over wireless networks under imperfect CSI. *IEEE International Conference on Communications Workshops (ICC WKSHPS)*, pages 1–6, 2021.
- Quoc-Viet Pham, Fang Fang, Vu Nguyen Ha, Md. Jalil Piran, Mai Les, Long Bao Le, Won-Joo Hwang, and Zhiguo Ding. A Survey of Multi-Access Edge Computing in 5G and Beyond: Fundamentals, Technology Integration, and State-of-the-Art. *IEEE Access*, 8, 2020.
- Xun Qian, Rustem Islamov, Mher Safaryan, and Peter Richtárik. Basis matters: Better communication-efficient second order methods for federated learning. *arXiv preprint arXiv:2111.01847*, 2021.
- Sashank J Reddi, Jakub Konečný, Peter Richtárik, Barnabás Póczós, and Alex Smola. Aide: Fast and communication efficient distributed optimization. *arXiv preprint arXiv:1608.06879*, 2016.
- Nicola Rieke, Jonny Hancox, Wenqi Li, Fausto Milletari, Holger R Roth, Shadi Albarqouni, Spyridon Bakas, Mathieu N Galtier, Bennett A Landman, Klaus Maier-Hein, et al. The future of digital health with federated learning. *NPJ digital medicine*, 3(1):1–7, 2020.
- Mher Safaryan, Rustem Islamov, Xun Qian, and Peter Richtárik. FedNL: Making Newton-type methods applicable to federated learning. *arXiv preprint arXiv:2106.02969*, 2021.
- Ohad Shamir, Nati Srebro, and Tong Zhang. Communication-efficient distributed optimization using an approximate newton-type method. In *Proceedings of the 31st International Conference on Machine Learning*, pages 1000–1008, 22–24 Jun 2014.

- Ruksar Sheikh, Mayank Patel, and Amit Sinhal. Recognizing mnist handwritten data set using pca and lda. In Garima Mathur, Harish Sharma, Mahesh Bunde, Nilanjan Dey, and Marcin Paprzycki, editors, *International Conference on Artificial Intelligence: Advances and Applications 2019*, pages 169–177, Singapore, 2020. Springer Singapore.
- Yuanming Shi, Kai Yang, Tao Jiang, Jun Zhang, and Khaled B. Letaief. Communication-efficient edge AI: algorithms and systems. *IEEE Communications Surveys Tutorials*, 22(4):2167–2191, 2020.
- Virginia Smith, Chao-Kai Chiang, Maziar Sanjabi, and Ameet Talwalkar. Federated multi-task learning. In *Proceedings of the 31st International Conference on Neural Information Processing Systems*, pages 4427–4437, 2017.
- Canh T. Dinh, Nguyen H. Tran, Tuan Dung Nguyen, Wei Bao, Amir Rezaei Balef, Bing B Zhou, and Albert Zomaya. Done: Distributed approximate newton-type method for federated edge learning. *IEEE Transactions on Parallel and Distributed Systems*, 2022.
- Madhusanka Manimel Wadu, Sumudu Samarakoon, and Mehdi Bennis. Federated learning under channel uncertainty: Joint client scheduling and resource allocation. In *2020 IEEE Wireless Communications and Networking Conference (WCNC)*. IEEE, 2020.
- Shusen Wang, Farbod Roosta-Khorasani, Peng Xu, and Michael W. Mahoney. GIANT: Globally improved approximate newton method for distributed optimization. In *Proceedings of the 32nd International Conference on Neural Information Processing Systems*, 2018.
- Han Xiao, Kashif Rasul, and Roland Vollgraf. Fashion-mnist: a novel image dataset for benchmarking machine learning algorithms. *arXiv preprint arXiv:1708.07747*, 2017.
- Hao Yu, Sen Yang, and Shenghuo Zhu. Parallel restarted sgd with faster convergence and less communication: Demystifying why model averaging works for deep learning. In *Proceedings of the AAAI Conference on Artificial Intelligence*, volume 33, pages 5693–5700, 2019.
- Jiaqi Zhang, Keyou You, and Tamer Başar. Distributed adaptive newton methods with global superlinear convergence. *Automatica*, 138:110156, 2022. ISSN 0005-1098. doi: <https://doi.org/10.1016/j.automatica.2021.110156>.
- Yuchen Zhang and Xiao Lin. Disco: Distributed optimization for self-concordant empirical loss. In *International conference on machine learning*, pages 362–370. PMLR, 2015.
- Yue Zhao, Meng Li, Liangzhen Lai, Naveen Suda, Damon Civin, and Vikas Chandra. Federated learning with non-iid data. *arXiv preprint arXiv:1806.00582*, 2018.
- Hangyu Zhu, Jinjin Xu, Shiqing Liu, and Yaochu Jin. Federated learning on non-iid data: A survey. *Neurocomputing*, 465:371–390, 2021.